

Computational Studies on a Solar Pond

*Thesis submitted in partial fulfillment for the requirements of the Degree
of Master of Chemical Engineering
Faculty of Engineering and Technology*

Thesis submitted by
Saswata Chakraborty
Master of Chemical Engineering
Examination Roll no: M4CHE22001
Registration Number: 153938 of 2020-2021

Under the guidance of
Dr. Parama Ghoshal
Assistant Professor
Chemical Engineering Department, Jadavpur University

JADAVPUR UNIVERSITY
KOLKATA-700032
INDIA

2022

DECLARATION OF ORIGINALITY AND COMPLIANCE OF ACADEMIC ETHICS

I hereby declare that this thesis contains literature survey and original research as a part of my *Master of Chemical Engineering* studies during academic session 2020-2022. I declare that this thesis has been written by me and in my own words, except for quotations from published and unpublished sources which are clearly indicated and acknowledged as such.

All information in this document have been obtained and presented in accordance with academic rules and ethical conduct.

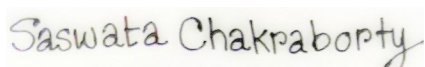
I also declare that as required by academic rules and ethical conduct, I have fully cited and referenced all materials and results that are not original to this work.

NAME: Saswata Chakraborty

EXAMINATION ROLL NUMBER: M4CHE22001

REGISTRATION NUMBER: 153938 of 2020-2021

THESIS TITLE: Computational studies on a solar pond

A handwritten signature in black ink that reads "Saswata Chakraborty". The signature is written in a cursive style and is placed on a light yellow rectangular background.

SIGNATURE

August 2022

CERTIFICATE

This is to certify that the thesis entitled “**Computational studies on a solar pond**” submitted by **Mr. Saswata Chakraborty** in partial fulfilment of the requirements for the award of the degree of **Master of Chemical Engineering** from Jadavpur University, Kolkata during the academic session 2020-2022 is a bona fide record of the project work carried by him under my supervision and this work has not been presented earlier for any other degree or diploma in any institute or university. The approval does not necessarily endorse or accept every statement made, opinion expressed or conclusion drawn as recorded in the thesis. It only signifies the acceptance of the thesis for the purpose for which it is submitted.

Dr. Parama Ghoshal

Project supervisor,
Assistant Professor, Chemical Engineering, Jadavpur University
August 2022

Prof. (Dr.) Rajat Chakraborty
Head, Chemical Engineering,
Jadavpur University,
Kolkata-700032
August 2022

Prof. (Dr.) Chandan Mazumdar
Dean, Faculty of Engineering and Technology,
Jadavpur University,
Kolkata-700032
August 2022

Acknowledgement

I would like to thank my professor and project supervisor, Dr. Parama Ghosal for giving me an opportunity to work on this project. This work has been allowing me to develop a deep understanding of Salt Gradient Solar Ponds, and also the immensely powerful and open source CFD software OpenFoam. Working on this has also allowed me to become comfortable while using the Linux operating system. I would also like to extend my gratitude to our HOD, Dr. Ujjaini Sarkar for allowing me to pursue this project.

At last, I would like to extend my heartfelt thanks to all my professors from the Department of Chemical Engineering, without whom I would have not developed the mental fortitude required to keep pursuing the project. Finally, I would like to thank my family and friends for their continuous support.

I feel extremely fortunate to have been allowed to pursue a project which has allowed me to be able to work and study within the safety of my home at this uncertain and dire phase of a Global Pandemic. I shall forever be grateful to God for the culmination of events for allowing me to pursue my project from such a well revered University.

Abstract:

Salt gradient solar pond is an environmentally friendly and sustainable method or rather a system to store solar energy in the form of heat energy. The solar pond is able to achieve this by utilising salt concentration gradient which prevents mixing of temperatures when a water body is heated due to solar radiation. As solar radiation falls on a water body it is absorbed in the layers of water, however the difference in temperature from the upper and the lower layer is nullified as the temperatures in the various layers intermix, and the temperature difference is lost. A Salt gradient solar pond has three zones: the Upper Convective Zone, with uniform temperature and concentration and is generally formed from fresh water or locally available water; below the Upper Convective Zone is the Non Convective Zone, which occupies almost half the depth of the pool, this zone has a salinity concentration gradient and subsequently a temperature gradient; the bottom Zone is termed as the Lower Convective Zone, which has the highest concentration and temperature and it serves as the main heat collection and thermal storage-medium. The inner workings of a solar pond is governed by equations of Temperature, Species and Momentum Transport. In this work a solver has been developed using OpenFOAM, for solving the governing equations of Temperature, Species and Momentum transport which dictate the behaviour of a Salt gradient solar pond. A thin square model of the Salt gradient solar pond has been made. The three zones of Lower Convective Zone, Non Convective Zone and Upper Convective Zone have been provided the height of 0.4m, 0.5m and 0.1m respectively. The solver is then executed for the model pond with three varying values of incident radiation 250W/m^2 , 500W/m^2 and 1000W/m^2 , varying values of Salt concentration in the Lower Convective Zone, and different boundary conditions for concentration at the bottom boundary of the Pond. It has further been tested against experimental data on Solar Ponds from published literature for validation.

Table of Contents:

	Topic	Page No.
1.	Introduction	7-10
1.1.	Some Facts Related to SGSP	11
1.2.	Applications of SGSP	11
1.3	Working Principle of Salt Gradient Solar Pond(SGSP)	11-12
2.	Literature Review	
2.1.	Salient Points From Literature Reviews	13-21
2.2.	Summary of Literature reviewed	22-31
3.	Methodology	
3.1.	Objective of the Project:	32-35
3.2.	Overview of OpenFOAM	36
3.3.	Development of the Solver for a Salt Gradient Solar Pond	37-40
3.4.	Initial and boundary conditions	40-42
3.5.	Courant Number	42-43
3.6.	Testing Grid Convergence	44
4.	Results and Discussion	
4.1	Validation of the Solver	45-48
4.2.	Temporal Evolution of Temperature With varying values of Incident Radiation	49-52
4.3	Comparison for Change in Temperature	53-54
4.4.	Temporal Evolution of Concentration With varying values of Salt Concentration and different boundary condition for salt at bottom	55-64
4.5.	Comparison and discussion for Change in Concentration	65-71
5.	Conclusion	72-74
6.	Nomenclature	75-76
7.	Appendix of Data Used	77
8.	References	78-83

1. Introduction:

Salt Gradient Solar Pond (SGSP) can be considered as an economical way of collecting and storing solar energy and utilising the same for low temperature processes mostly within the range of 70°-80°C. The SGSP may be used as a thermal energy reservoir for applications which require a continuous supply of heat ([Tabor, 1981,1980](#)) [1][2]. The SGSP is unique as this does not have convective currents throughout the length as in case of other ponds. The salt water forms a vertical salinity gradient in which low-salinity water floats on top of the high-salinity water. The layers of salt solution increases in concentration (and therefore in density with depth). Below a certain depth the solution has a uniformly high salt concentration ([Osamah A.H. AL-Musawi et.al., 2020](#)) [3].

There is an urgent need for providing an economically viable solution for storage and utilisation of solar energy especially in the continent of Africa. SGSP can be considered as an easy and feasible alternative for individuals requiring thermal heat storage option. The main advantage of SGSP is the lack of complicated mechanical setup and independence from regular maintenance. Solar ponds are able to retain the temperature during the night time as well as remain in operation during the entire year. Utilisation of solar ponds across the globe has pointed out that its use can reduce the expenditure on the processes which depend on thermal energy utilisation.

Solar ponds are very simple to set up and they are able to maintain a very good thermal energy storage due to the concentration gradient that is set up during the construction of the same. The only main requisite for setting up solar pond is the requirement of a large area which is available mainly in barren areas, hence these can be used to help in establishing industries on a small scale which will help in economic upliftment of the same. Also the main materials required in the construction of solar ponds is insulation material which has to be used as a liner for the sides and the base. Insulation materials required for the construction of solar ponds are not very expensive and are relatively resistant to degradation so a one time investment can lead to long term economic sustainability. The salt required for construction a solar pond in establishing the salinity gradient is a readily available raw material as the salt which is to be used need not be of the grade of table salt but rather raw salt extracted directly from the sea maybe use utilised.

The only danger is the intermixing of layers due to the entry of a large foreign particle or the lower convection zone reaching extremely high temperature causing boiling. The problem of introduction of a large foreign particle can be avoided by isolation of the solar pond by constructing it in a area away from human and animal traffic. The problem of intermixing due to boiling phenomena in the lower convection zone can be eliminated by ensuring regular removal of heat.

Heat energy generation is a very costly endeavour for any industry and even slight reductions in cost for heat energy generation can lead to good economic profit. Also, since solar ponds operate by utilisation of solar energy so that energy which is generated by solar gradient solar ponds is completely free barring the cost of construction which is also quite minimal. Currently a lot of large scale solar ponds have been set up all over the world and they have proven to be quite efficient in operation.

It has been a continued effort by various researchers in understanding the principles of working and means of improvement of solar ponds so that they can be made even more efficient and profitable. The researches and experiments have broadly been conducted into two main categories one in which the principle of working itself has been investigated and models have been developed on that basis to generate a deeper understanding of the same, secondly a lot of experiments have been conducted to test how the performance of the solar pond can be further improved by means of variation in geometry and addition of materials inside the solar pond. This process of experiments and analysis is continuous and these are being carried out everyday. The main objective of making the solar pond more economically feasible and efficient is an ongoing effort.

Although the role of solar ponds have been very minimal till date however with the need for reduced dependence on fossil fuels currently becoming a norm, due to

depletion of fossil fuel reserves in the near future and the alarming rise of global temperature levels, the importance of solar ponds and their viability can no longer be ignored. As time progresses it is becoming increasingly clear that solar energy is the way for sustainable future and since solar ponds are able to tap into this energy directly it will help in ensuring a better tomorrow.

Overtime it has been observed that solar ponds have a lot of versatility in the energy that they can generate as the stored heat energy has numerous uses. As the efficiency of solar ponds increase the available energy from it will also continue to grow and it will be able to provide much higher energy output in the near future.

On comparison with a commercially available solar cell which has an efficiency of 14 to 15%, a solar pond has a similar efficiency value. However as the construction of solar pond does not require expensive materials and big industrial setup hence, it can be considered a good alternative to solar cells when the objective is to obtain heat energy. The heat energy developed inside the solar pond can be used to generate electricity using an organic rankine cycle. The only drawback of a salt gradient solar pond is the necessity for it to be constructed over the large area. This issue will be mitigated, when farther research and experiments will allow us to improve the efficiency of solar ponds. Taking in account all the above considerations it can be concluded that a SGSP is indeed a viable setup for converting solar energy to heat energy and storing the same.

1.1. Some Facts Related to SGSP:

- First SGSPs were constructed in Israel in the early sixties by Tabor and his co-workers. A maximum temperature of 100°C was obtained at the bottom, many practical difficulties were encountered and the work was abandoned([Tabor, 1981,1980](#)) [1][2].
- Number of SGSPs have been built all around the world to utilize the stored heat for providing process heat and generating power
- The Largest SGSP: Installed at Beit Ha'aravah in Israel (area of 250000 m²). Heat is used to generate electricity using an Organic Rankin Cycle.

1.2. Applications of SGSP:

- Desalination([Rostamzadeh et al., 2019](#)) [4] and Brine management([Agha et al., 2001](#)) [5].
- In Australia SGSP is used to supply heat in Salt Production Process at Pyramid Hill.
- In India, the Largest SGSP (about 6000 m²)has been built at Bhuj, Gujarat (used to supply process heat to a dairy farm).

1.3. Working Principle of Salt Gradient Solar Pond(SGSP):

A SGSP has three zones: the Upper Convective Zone(UCZ), which has a thickness of 10-20 cm, with uniform temperature and concentration and is generally formed from fresh water or locally available water; below the UCZ is the Non Convective Zone (NCZ), which occupies almost half the depth of the pool, this zone has a salinity

concentration gradient and subsequently a temperature gradient; the bottom Zone is termed as the Lower Convective Zone (LCZ), which has the highest concentration and temperature and it serves as the main heat collection and thermal storage medium.

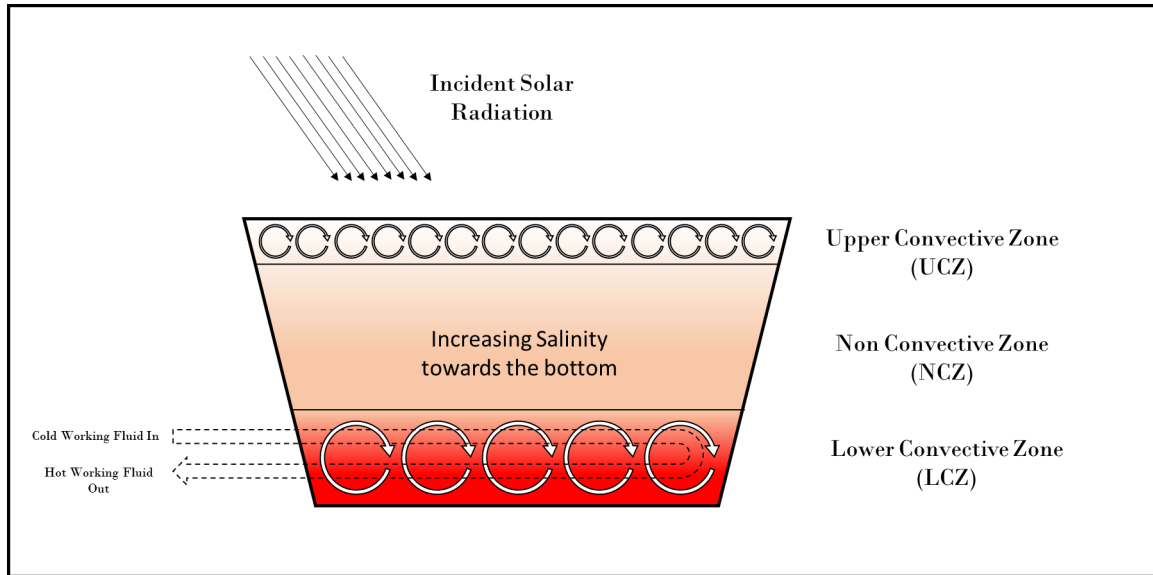


Figure 1. Schematic of Salt Gradient Solar Pond

The concentration gradient in the NCZ also establishes a density gradient and this is the fundamental factor in allowing the SGSP to absorb and store thermal energy from solar radiation, as density gradient suppresses convective currents (arising due to temperature and concentration profiles) to within the UCZ and LCZ and inhibit convective current and mixing throughout the depth of the SGSP. The Resultant temperature gains within the LCZ is significant which may be utilised for multiple uses. It is to be noted that density will dominate over both temperature and concentration driven driving force and heat loss by conduction will be negligible as water is good insulator ([Ganguly et. al., 2019](#)) [6]. Losses to the surroundings via the Walls of the SGSP will be controlled by the use of thick durable liner especially in the LCZ ([Beiki et. al., 2020](#)) [7] .

2.Literature Review:

2.1.Salient Points From Literature Reviews:

	YEAR	AUTHOR	TITLE	SALIENT POINTS
1.	2015	Hua Wang , Xiaolei Yu , Feiling Shen , Liugang Zhang	A Laboratory experimental study on effect of porous medium on salt diffusion of salt gradient solar pond	<p>1. Blank Test results in the highest salinity.</p> <p>2.NCZ salinity with porous medium is the least, indicating highest stability.</p> <p>3.Lesser the porosity of the porous medium, lesser the diffusion of salt to higher levels of SGSP</p>
2.	2018	Hua Wang, Liu Gang Zhang and Yan Yang Mei	Investigation on the exergy performance of salt gradient solar ponds with porous media	<p>1. Exergy evaluated for NCZ and LCZ, tested against Exergy of solar radiation.</p> <p>2.The proximity of NCZ to the atmosphere causes lesser variation among the test cases used.</p> <p>3. Steeper temperature gradient damages the stability of SGSP.</p>
3.	2017	Mohamad Aramesh , Alibakhsh Kasaeian , Fathollah Pourfayaz , Dongsheng Wen	Energy analysis and shadow modeling of a rectangular type salt	<p>1. MVT for definite integrals has been applied to evaluate highly transient parameters.</p>

			<p>gradient solar pond</p>	<p>2. Objective is to utilise curve fitting methods to remove the need for integration.</p> <p>3. Shadow effect due to vertical walls and the azimuthal angle has been evaluated using trigonometric relations.</p>
4.	2017	Asaad H. Sayer, Hazim Al-Hussaini, Alasdair N. Campbell	<p>An analytical estimation of salt concentration in the upper and lower convective zones of a salinity gradient solar pond with either a pond with vertical walls or trapezoidal cross section</p>	<p>1. mathematical Expressions developed in agreement with current experiment and previous work.</p> <p>2. Lesser effect of wall inclination on LCZ concentration, as compared to the UCZ concentration.</p> <p>3. As inclination reduces UCZ concentration becomes lower.</p> <p>4. A pond with inclined walls will take greater time to achieve uniformity.</p> <p>5. Linear profile in NCZ concentration becomes weaker with reducing wall inclination for</p>

				the trapezoidal case.
5.	2016	Cristóbal Silva, Daniel González, Francisco Suárez	An experimental and numerical study of evaporation reduction in a salt gradient solar pond using floating discs	<p>1. LCZ temperature does not increase with coverage, which is attributed to reduced NCZ thickness causing a steeper gradient leading to greater heat loss.</p> <p>2. Increase in UCZ temperature due to evaporation suppression and this causes an increase in overall thermal energy stored.</p> <p>3. Due to changes in layer thickness moving interfaces develop.</p> <p>4. fraction of radiation that penetrated the water surface decreases till 70% coverage however an increase is observed afterwards.</p> <p>5. Although LCZ temperature is unaffected the thickness increases indicating greater energy stored.</p>
6.	2017	Howard O. Njoku, Boniface E. Agashi, Samuel O. Onyegegbu	A numerical study to predict the energy and exergy performances of a	<p>1. The Model developed is evaluated explicitly.</p> <p>2. Temperature obtained in</p>

			<p>salinity gradient solar pond with thermal extraction</p>	<p>presence of extraction was minimum.</p> <p>3. Highest temperature was obtained in the LCZ while the lowest was observed in the UCZ.</p> <p>4. NCZ observed to have significant heat storage capacity.</p> <p>5. Energy efficiencies evaluated will always be higher than exergy efficiency due to the irreversibility introduced in the various layers of SGSP.</p>
7.	2014	Hua Wang, Jianing Zou , J.L. Cortina , J. Kizito	<p>Experimental and theoretical study on temperature distribution of adding coal cinder to bottom of salt gradient solar pond</p>	<p>1. Analysis of Stability of NCZ using thermal and saline Rayleigh number.</p> <p>2. Experimental temperature gain is observed to be lesser than that predicted by numerical model, this is attributed to the difference in the thermal properties of mixture of coal cinder and saline water; as compared to only saline water.</p>

				<p>3. Comparative study with pebble at the bottom, indicates faster gain and loss of temperature which shows a greater absorption affinity of coal towards solar radiation.</p>
8.	2018	Khadije El Kadi, Sherine Elagroudy, Isam Janajreh	<p>Flow simulation and Assessment of Salinity Gradient Solar Pond Development</p>	<p>1. Utilisation of multi-species, high fidelity CFD model</p> <p>2. Solar radiation not considered, BC's defined by fixing patch temperatures</p> <p>3. A set up of pressure linked conservation equations are used, which are solved using SIMPLE method.</p> <p>4. Fick's law is used to describe inter-layer diffusion of salt as zero mixing has been assumed initially in between the layers.</p> <p>5. Most stable Temperature Gradient was observed in the NCZ for lowest LCZ concentration whereas it yielded the most stable Salinity Gradient</p>

				in the NCZ.
9.	2018	Qi Wu, Hua Wang , Shukuan Xie, Liugang Zhang, Jie Wang, Zhanwei Dong and Tao Zhao	Effect of heat extraction on the thermal efficiency of salt gradient solar pond	<p>1.SGSP shows improvement in thermal efficiency when he takes traction is involved.</p> <p>2. Temperature of LCZ and NCZ both is reduced the gradient is stabilized (becomes less steeper).</p> <p>3. Also, reduction in temperature due to heat extraction, will reduce the temperature difference with the surroundings and hence reduce heat loss due to ambience as is the case with is SGSP without heat extraction.</p>
10.	2020	Shyamal G. Chakrabarty, Uday S. Wankhede, Rupesh S. Shelke, Trushar B. Gohil	Investigation of temperature development in salinity gradient solar pond using a transient model of heat transfer	<p>1.A mathematical model for SGSP has been developed and it has been solved using hte finite difference method</p> <p>2.The values of density and specific heat are considered to be constant for LCZ and UCZ & the heat stored in NCZ has not been considered.</p> <p>3. Multiple parameters (namely individual zone thickness and shading effects have been varied</p>

				<p>to test its effects to test its effects on LCZ temperature</p> <p>4.Selection of thickness of esch zone is made on the basis of highest LCZ temperature and quickest warm-up time.</p> <p>5.Effect of NCZ thickness on LCZ temperature is dependent on thermophysical properties of the ground.</p> <p>6.LCZ temperature is strongly dependent on LCZ & NCZ thickness, and even though evaporation loss in UCZ is found to be significant, the effect on LCZ temperature is insignificant.</p> <p>7. The effect of shading area is insignificant on SGSP of very large surface area (over 10000m²)</p>
11.	2014	Jeffrey A. Ruskowitz, Francisco Sua´rez, Scott W. Tyler , Amy E. Childress.	Evaporation suppression and solar energy collection in a salt-gradient solar pond	<p>1.Covers over SGSP and the corresponding effects on supressing evaporative losses.</p> <p>2.Investigation of Temperature evolution of SGSP resulting due to use of covers and validation</p>

				<p>against pre established mathematical model.</p> <p>3.Performance analysis of three types of covers, namely continuous, floating discs and hemispheres.</p>
12.	2018	Shahram Derakhshan, Seyedeh Elnaz Mirazimzadeh, Syamak Pazireh	Study of Buoyancy-Driven Flow Effect on Salt Gradient Solar Ponds Performance	<p>1. 1-D and 2-D numerical model of SGSP simulated and analysis performed to investigate unsteady buoyancy driven flow induced inside SGSP</p> <p>2. The 1-D numerical method was utilised to carry out thermal analysis with regard to layer thickness, using energy conservation equation.</p> <p>3. The 2-D analysis using CFD is for stability study.</p>
13	2004	M.R. Jaefarzadeh	Thermal behavior of a small salinity-gradient solar pond with wall shading effect	<p>1. establishes a relation between Shading area, and the reduction in sunny area and consequently the temperature of LCZ</p> <p>2. A robust correlation for attenuation of solar radiation inside the SGSP.</p>

				3. Utilisation of daily average irradiation values
14	2015	Ridha Boudihaf	Numerical temperature and concentration distributions in an insulated salinity gradient solar pond	<p>1. Dimensionless governing equations are solved by finite-volume method using SIMPLER algorithm with HYBRID scheme to study the behaviour of temperature and concentration gradients.</p> <p>2. Simplification of the analysis with assumptions which does not violate the fundamental principles of SGSP</p> <p>3. Effect of Buoyancy ratio on the Increase and decrease of concentration and Temperature in the LCZ and UCZ.</p>
15	2004	M. M. Ould Dah,, M. Ouni, A. Guizani, A. Belghith	Experimental Study of the evolution of temperature and salinity profiles in a salinity gradient solar pond	<p>1. Experimental Setup for evaluating the Temperature and Concentration Gradient</p> <p>2. Complete control over Initial concentration Gradient and Constant Radiation Source for the entire length of the experiment.</p> <p>3. Molecular Diffusion of salt occurs from LCZ to UCZ throughout the entire length of the experiment</p>

2.2. Summary of Literature reviewed:

Through experimentation to study the effect of porous media(PM) on SGSP ([H. Wang et. al., 2015](#)) [8] it is observed that upon addition of porous materials to the LCZ, it develops two separate layers, one with a mixture of the medium and salt water & a salt water layer on top of the said layer. As salts spread upwards to form the the gradient in the NCZ, sampling has been carried out at varying lengths over time, with a setup consisting of different porosity materials & a blank set-up without using porous medium (PM). It is known (has been researched) that PM improves temperature and stability of the NCZ & the stability of the SGSP. The Blank test result yields the highest salinity at lower depths, which may be accounted for due to the inability of taking samples from within the porous medium crevices, without disturbing the setup irreparably. However, with the passage of time it has been observed that salinity in the NCZ with the porous media is smaller than the blank indicating greater binding capacity of porous media and hence reducing diffusion of salt to the upper layer. It is observed that the smaller the porosity is, higher is the ability for the medium to prevent diffusion of salt to the higher layers. Calculation of salinity diffusion coefficient indicated a more stable value for the blank, some negative values were obtained while using the porous media which may be due to Soret effect. So, the porous medium added reduces salt diffusion and the highest salinity of blank at the bottom is attributed to salt water trapped in holes and lesser the porosity higher will be the ability of the medium to prevent diffusion so in turn stabilizing it.

Investigating the exergy performance of SGSP with the same PM([H. Wang et al., 2018](#)) [9] aimed to establish, both experimentally and theoretically the Exergy performance of SGSP when PM is added to the LCZ. Three setups have been used with one blank and two others with varying PM components namely cinder and a combination of cinder and cobblestone. The laboratory utilised is well insulated and a PLC scheme has been utilised to simulate sunlight pattern. It is to be noted that due to low temperature of the UCZ, this zone has not been analysed. Exergy, a state parameter, with temperature data based calculation, accumulated from experimentally measured results. The Exergy values are evaluated for NCZ & LCZ, and the efficiency is measured against the Exergy of solar radiation modified from [Petela\(Giestas et al., 1996\)](#) [10]. To avoid instability of NCZ, the experiment period only lasts 5 days and the measurement points are not identical but the data is considered sufficient to show temperature distribution in the SGSP. It is observed that, without energy extraction, Exergy increases the highest for setup with PM with both cobblestones and cylinder, when it is evaluated using mean temperature data (daily). The temperature trend points to highest temperature gains in the LCZ and cobblestone and cinder combinations domination over the other cases. The lower difference among the cases in NCZ is attributed to its proximity to the atmosphere. However it is important to consider

- i. The case with the highest temperature is damaged by the fifth day due to steeper gradient

ii. As SGSP temperature increases the Exergy loss will increase with data revealing drop in efficiency as experiment proceeds. The mean daily Exergy efficiency of setup of cobblestone and cinder is the highest among the three with same size of LCZ and PM. it also kills higher temperature and heat Exergy in the LCZ. This may be concluded as reasonable selection of PM and combination of materials in PM will improve the Exergy property of SGSP and this combination may be tested with different components to further optimise the output from a SGSP.

In a similar study, effect of addition of coal to the LCZ of SGSP was compared against test cases of untreated bottom layer and a dark bottom surface SGSP ([H. Wang et. al., 2014](#)) [11]. A numerical model was established and the the boundary condition data utilised was taken from the experimental cases. Another set of data was obtained where coal cinder was replaced with pebbles. It was observed; LCZ reaching the highest temperature for coal cinder, followed by table and other cases full stop the increase had the potential to destroy the NCZ, and so it was analysed using thermal and saline Rayleigh number, and the stability number was found to be within the critical stability condition established in earlier papers. The one-dimensional transient model utilised to simulate the experiment was solved using the finite difference method. The resulting curves from the data obtained from the experiment and the numerical model showed similar Trend and good consistency. Some inconsistencies in data obtained during morning and afternoon have been did

used to have been resulted from convective thermal heat resistance between solid base and PM contact, which simplifies the effective thermal conductivity and this caused arbitrary heat loss. A similar analysis in a larger SGSP, showed reduced gain in LCZ as compared to predictions by model, which is attributed to thermophysical properties of mixture of coal cinder and saline. The experiment successfully demonstrates the ability of coal cinder to increase thermal performance of SGSP and provides a reliable simulation model which may be used for prediction in larger cases. The economic viability due to cheap availability of coal cylinder is to be considered.

An Energy analysis and shadow modelling study has been undertaken ([M. Aramesh et. al., 2017](#)) [12] to remove a major restriction of the momentary or rather temporary usability of existing equations of SGSP energy analysis and the large bulk of calculations involved in utilising such equations when large time periods are involved. Also the shading effect which influences the energy storage performance has been analysed. The parameters involved in calculating the energy entering the pond at any given depth are dependent on angle of incidence of solar radiation and if they are to be integrated a large degree complexity is faced. To remove this complexity mean value theorem for definite integrals have been applied to the parameters, transmissivity due to reflection and transmissivity due absorption using curve fitting methods and the results are found to be satisfactory with low degree of error. The objective is to remove the integration by using simple multiplication of the

mean values evaluated for the parameters. Further the shadowing effect of vertical walls have been investigated which is a result of the azimuthal angle and this has been established numerically using trigonometry. The Shadow effect has been incorporated into the final calculation for energy available at a depth. The specifications and data utilised have been taken from an actual functioning SGSP. The final theoretical results have been tallied with experimental findings on the same pond. It has been made possible by comparing the efficiency of the LCZ layer which is the ratio of energy stored to energy availability. The theoretical efficiency are found to be quite close to the experimental results. Hence this method may be considered successful in predicting the amount of energy entering the pond.

A study for analytical estimation of salt concentration in the upper and lower convective zones of salinity gradient solar pond with either a pond with vertical walls or trapezoidal cross section

[\(A.H. Sayer et al., 2017\)](#) [13] establishes straight forward analytical formula for evaluating concentration of UCZ & LCZ, using an experimental setup to validate the calculations. The derived equations are only dependent on thickness of layers and salt diffusivities and would allow for accurate maintenance time prediction for SGSP and also in designing them. Models for SGSP with both vertical and trapezoidal walls were developed and tested against experimental case for the vertical wall scenario while for the incline wall comparisons were made against an experiment established previously, [\(Karim et al., 2010\)](#) [14]; both the comparisons indicated satisfactory fit

of the analytical data with that of experimental ones. Upon closer analysis of the established equation it is observed that inclination of pond walls have a higher influence on UCZ concentration increases with respect to LCZ concentration increase. The inclination is varied multiple times to check its effect on concentration of UCZ and LCZ; further strengthening the fact that it has significant effect on UCZ (which is as a result of lowering LCZ volume with greater incline). This final analysis also shows that attainment of uniformity and strong linearity of concentration of NCZ with higher inclination of the pond walls.

To investigate temperature development of SGSP, namely that of LCZ with parameters ranging from individual zone thickness to ambient losses and shading effects, a numerical study has been conducted utilising a transient model of heat transfer solved using a finite difference method ([S.G. Chakrabarty, et. al., 2020](#)) [15]. The model has been developed and validated by comparison with experimental data. LCZ temperature is strongly dependent on LCZ & NCZ thickness, and the effect of NCZ thickness is further dependent on thermal conductivity of ground and the depth of water table. While, the effect of UCZ thickness is minimal, although evaporation loss is significant.

To mitigate the issue of evaporative losses in SGSP different cover types are utilised and compared to obtain corresponding effects on suppressing evaporative losses and Temperature evolution of SGSP ([J.A. Ruskowitz, et al.,2014](#)) [17]. The decreased

photon penetration increases the warm-up time of the LCZ. Continuous plastic cover demonstrates the highest reflective loss however it has the highest suppression capability against evaporative losses due to ease of water pooling on the continuous sheet. Although, covers restrict light the ability to reduce evaporative losses and hence in turn restricting heat loss via evaporation overcomes this issue. Among, the three varieties of cover used, namely: continuous plastic sheet, floating discs and floating hemispheres, floating discs are the most transparent and hence result in the highest temperature gain of the LCZ.

An effort is made to study the effect of evaporation reduction in SGSP using floating discs ([C. Silva et. al., 2017](#)) [18]. It is observed that a two-fold advantage is obtained, one being reduction in evaporation loss, and second being increased thermal storage inside the is SGSP. During the course of the experiment the effect of floating this on attenuation coefficient is found to be relatively manageable. The increased thermal storage observed is attributed to two factors, increase in temperature of UCZ due to evaporation suppression and, due to increase size of LCZ allowing greater radiation to pass through it. The NCZ layer thickness reduces on increase of coverage obtained by EC observations. This study shows major economic benefits which is two fold on using transparent covers on SGSP.

To predict the energy and exergy performances of a salinity gradient solar pond with thermal extraction a one dimensional numerical model has been developed ([H.O.](#)

[Njoku et al., 2017](#)) [19] for establishing time varying temperature profiles in a SGSP, while incorporating provisions to account for thermal extraction in the LCZ. The model is used to investigate parameters such as energy efficiency, exergy efficiency and irreversibility. During the simulation period, which is designed to emulate a time period of three years, parameters such as extraction rate and depth of LCZ and NCZ have been varied to study the subsequent effects. Predictable temperature outcomes were observed with the highest temperature in LCZ and least in UCZ, and reduction in temperature as a result of heat extraction. Rates of thermal energy and exergy storage is maximum initially and it wanes later, due to heat extraction, this later follows the trend of available solar radiation. Irreversibilities are observed to be released in NCZ, while higher values are obtained for LCZ and UCZ, due to greater avenues for entropy generations. LCZ has the highest energy storage, but NCZ also shows significant heat storage capabilities. On analysing thermal performance of LCZ with heat extraction, it is found that overall energy efficiency is greater than exergy efficiency by order of magnitude, and both values converge with time, overall efficiency is always greater than extraction efficiency. Further the energy and exergy performance of SGSP cannot be improved by increasing thermal extraction from LCZ, but there is a limit, as extraction is increased, the temperature in LCZ falls and the gradient in NCZ becomes steep which may cause instability. This greater insight is obtained by incorporating exergy analysis in the study of SGSP.

Similarly, setting up competitive cases of experimental SGSP with provisions for

heat extraction in one case ([Wu et al., 2018](#)) [20]. Significant improvement in thermal efficiency is observed in the case where heat extraction is available, as the heat extracted using an exchanger arrangement is a term which complements the heat stored in the efficiency expression which has been utilised. Also a gain in total heat stored it is concluded which is due to the fact that, as the temperature difference with the surrounding is reduced due to heat extraction, heat losses are reduced. To further advantages observed are the stabilization of the gradient in the NCZ layer and also a reduction in temperature of NCZ interface, which, on extraction of heat from LCZ causes a reduced temperature difference reducing the driving force and hence, improving stability. Hence, heat extraction helps in improving the temperature control of SGSP, and the enhanced heat storage resulting from it prolongs the life of SGSP.

Due to the presence of multiple gradients inside of various layers of SGSP some buoyancy driven flows are expected, a study has been carried out to analyse this behaviour ([Shahram et al., 2018](#)) [21]. This study involves both 1-D and 2-D models to analyse both thermal performance and stability of the SGSP. The result of 1-D study concludes that a longer NCZ layer improves temperature gain of LCZ. The 2-D model indicated that sharp gradients in NCZ will destabilize the SGSP as it will not be able to inhibit buoyancy driven flows across the layers. This will also reduce the temperature of LCZ as heat energy will be lost to the upper layers more readily.

To compensate for lack of the analysis study of progressive development of zones of diffusion and establishment of temperature and salinity gradient across the wiring layers of SGSP, high-resolution, multispecies non-isothermal CFD analysis has been undertaken ([Khadije El Kadi et. al., 2019](#)) [22]. On setting up required mesh and boundary conditions, localised inter facial data has been obtained allowing for a closer analysis of gradients developing across NCZ and temperature information about LCZ. The radiation input has been simulated via patching all three zones with prescribed temperatures and similar approach was carried out for salinity. The simulations were carried out for 6 hours of real time, and velocity conditions obtained, validated currents in UCZ and LCZ , and none in in NCZ. Density difference may be considered as the cause of localised motion, and higher rates of diffusion are obtained at the interface of the three zones. It is finally observed that the most stable temperature gradient is obtained for the lowest concentration of LCZ while the most stable salinity gradient is obtained for the highest salinity concentration LCZ.

3. Methodology

3.1 Objective of the Project:

The work involves generating a Robust Solver for the transport equations (using a finite volume strategy) which govern the SGSP, using OpenFoam an open Source CFD software package, to allow us to analyse and simulate the behaviour of the SGSP. Under varying conditions of incident radiation and initial salt concentration in the LCZ.

It can be considered that the fluid flow in SGSP follow the following conservation laws of continuity, species transport, x- and y- momentum, and energy which can be represented as the following Governing equations:

Mass balance:

$$\nabla \cdot \vec{V} = 0 \text{-----(1)}$$

Momentum balance:

$$\rho_o \left[\frac{\partial (\vec{V})}{\partial t} \right] + (\vec{V} \cdot \nabla) \vec{V} = -\nabla p + \rho \vec{g} + \mu \nabla^2 \vec{V} \text{-----(2)}$$

Density is expressed as functions of temperature and salt-concentration with Boussinesq approximation

$$\rho(C, T) = \rho_o [1 - \beta_T (T - T_o) - \beta_C (C - C_o)] \text{-----(3)}$$

where, ρ = density at temperature T and salt-concentration C [kg/m³]

ρ_o = density at reference temperature T_o and reference salt-concentration

$$C_o$$

β_T = volumetric thermal expansion coefficient

β_c = solutal expansion coefficient

Energy balance:

$$\frac{\partial T}{\partial t} + \vec{V} \cdot \nabla T = \alpha \nabla^2 T + S \text{-----(4)}$$

where α : thermal diffusivity,

S : thermal source term; solar radiation is added as thermal source term.

Species balance:

$$\frac{\partial C}{\partial t} + \vec{V} \cdot \nabla C = D \nabla^2 C \text{-----(5)}$$

Equation is for the evaluation of Solar Radiation:

The angle of incidence of direct radiation to a horizontal plane with normal (zenith angle) is given by Duffie and Beckman, 1980[23]

$$\cos(\theta_i) = \cos(\delta) \cos(\Phi) \cos(\omega) + \sin(\delta) \sin(\Phi) \text{-----(6)}$$

where,

δ : angle of declination

Φ : the angle of latitude

ω : the hour angle

The declination angle δ is defined in degrees by

$$\delta = 23.45 \sin \left(\frac{360 (284 + n)}{365.25} \right) \text{-----(7)}$$

where n is the day of the year

The hour angle is

$$\omega = \frac{2 \pi (h - 12)}{24} \text{-----(8)}$$

where h is local time

The hour of sunrise is given by

$$h_s = 6 + \frac{12}{\pi} \arcsin (-\tan \phi \tan \delta) \text{-----(9)}$$

and, the day-length is obtained

$$L_D = 6 + \frac{24}{\pi} \arccos (-\tan \phi \tan \delta) \text{-----(10)}$$

Attenuation of Solar Radiation entering the pond

The radiation entering the pond surface is given by

$$I_s = (1 - R) I \text{-----(11)}$$

where R is the coefficient of Reflection given by Wang and Akbarzadeh, 1983[24]

$$R = \frac{1}{2} \left[\frac{\sin^2(\theta_i - \theta_r)}{\sin^2(\theta_i + \theta_r)} + \frac{\tan^2(\theta_i - \theta_r)}{\tan^2(\theta_i + \theta_r)} \right] \text{-----(12)}$$

where θ_i is the angle of incidence, θ_r is the angle of refraction, and

$$\sin \theta_i = n \sin \theta_r \text{-----(13)}$$

where n is the index of refraction (n = 1.33 for water).

Inside the pond, The solar radiation is reduced exponentially with depth as energy is absorb by the fluid layers. The rate of decay or transmissivity is a function of the

wavelength of the radiation and for the whole spectrum of wavelengths can be expressed as Rabl and Nielsen, 1975[25]

$$\tau = \sum_{j=1}^4 \eta_j \exp\left(\frac{-\mu_j Z}{\cos(\theta_r)}\right) \text{-----(14)}$$

Akbarzadeh and Ahmadi 1980[26], have further shown the effects of salt concentration, water turbidity and bottom and wall reflection on the reduction of absorbed radiation in a coefficient of $\theta_0=0.8$. Considering the value of θ' to be 0.85, on multiplication with (1-R) shows a close match with the value of θ_0 .

So finally the modified equation becomes

$$I_R = (1-R) \theta' \tau I \text{-----(15)}$$

while the derivative is

$$\frac{dI_R}{dZ} = (1-R) \theta' I \left(\frac{\partial \tau}{\partial Z} \right) \text{-----(16)}$$

These two parameters are correlated to the Source term in the energy equation, as

$$Q_R = (A) I_R \text{ for the LCZ, and } E(Z,t) = \frac{-d}{dZ} [I_R(Z,t)] \text{ for the LCZ (M.R. Jaefarzadeh , 2004)}$$

[27]

3.2. Overview of OpenFOAM :

OpenFOAM is a Free Open Source Software. It is written in C++. It originates from Imperial College London and it is widely used FOSS for CFD. It has a large user base across most areas of engineering and science, from both commercial and academic organisations. OpenFOAM has an extensive range of features to solve anything from complex fluid flows involving chemical reactions, turbulence and heat transfer, to acoustics, solid mechanics and electromagnetics. The core difficulty or rather challenge lies in acclimatizing with the OpenFoam software to the extent where it is possible to develop codes which allow for the solution of Coupled Transport Equations. This difficulty arises due to the limitations of OpenFoam which are, a lack of a graphical user interface(GUI) and lack of robust documentation. Attaining proficiency with OpenFoam will rely on reverse engineering codes for solvers provided as examples in the software package itself and a lot of trials to establish and refine the code. However, working with OpenFoam has its advantages, most notable of which is its open source nature allowing unlimited modifications to be made and the ready availability on multiple platforms without any price or server based restrictions, both of which are unavailable on commercially available CFD software packages.

3.3. Development of the Solver for a Salt Gradient Solar Pond:

OpenFOAM inbuilt solver dose not have the capability to handle species balance equation therefore it is required to develop a solver to accommodate the species concentration equation([M.Chakkingal, et. al., 2020](#)) [28].The required solver is developed by modifying the existing solver

the `buoyantBoussinesqPimpleFoam` where the Boussinesq correlation for temperature, $1.0 - \beta \cdot (T - T_{ref})$, is modified to incorporate both the changes in temperature and concentration . Additional changes are incorporated to the solver for establishing its ability to solve the Species balance equation. This involves the following steps:

1. A new header file is created containing the Concentration equation in the `buoyantBoussinesqPimpleFoam`, conveniently named `CEqn.H`.
2. This Header File contains the transport equation for Concentration as per Equation (5), as : `fvm::ddt(C) + fvm::div(phi, C)- fvm::laplacian(Diff, C) == 0`
3. As this is a new Scalar which is being introduced to the solver, the information must be updated in the `createFields.H` Header File.
4. The same `createFields.H` Header File, already contains a Temperature based Boussinesq correlation, which is to be modified to account for changes in concentration as Equation (3).
5. A new correlation is established in `createFields.H` as $\rho C = 1 + \beta_c (C - C_o)$, and the ρC is added to the $(p_{rgh} + \rho k \cdot gh)$ as $(p_{rgh} + \rho k \cdot gh + \rho C \cdot gh)$.
6. While incorporating the Concentration equation, and its subsequent effect on

the Boussinesq correlation, three new parameters are introduced namely Diffusivity D , thermal contraction coefficient β_c and a reference salt concentration C_o .

7. The parameters D , β_c and C_o have to be incorporated into the code; in the `readTransportProperties.H` header file.
8. Changes have to be made in the `pEqn.H` to accommodate the ρC , where $p = p_{rgh} + \rho k * gh$; must be changed to $p = p_{rgh} + \rho k * gh + \rho C * gh$. Also, in the same file $p_{rgh} = p - \rho k * gh$; must be changed to $p = p_{rgh} + \rho k * gh + \rho C * gh$.
9. In the `Ueqn.H` header file, the ρC must be incorporated in to the `pimple.momentumpredictor` loop.
10. To ensure that the concentration equation is solved simultaneously with the Momentum and Temperature Equation, `Ceqn.H` is added to the main Solver file, `solarPond.C` file inside the loop as `#include Ceqn.H`.
11. Finally the Solver is compiled as per rules of OpenFOAM, and investigation carried out if an error message is received. This process is repeated until no further errors are discovered and the code compiles successfully.

For testing the solver a thin square model of the SGSP has been made with both the height(H) and length(L) of 1m as shown in the figure. The three zones of LCZ, NCZ and UCZ have been provided the height of 0.4m, 0.5m and 0.1m respectively. However, some Complications may arise due to the various processes occurring in an out of the salinity gradient solar pond, which is highlighted by studies of transient

behaviours of hydrodynamic, heat and mass transfer in the solar pond. So some assumptions are made for simplifying the analysis of the model as per [Ridha Boudihaf, et. al., 2015.\[29\]](#).

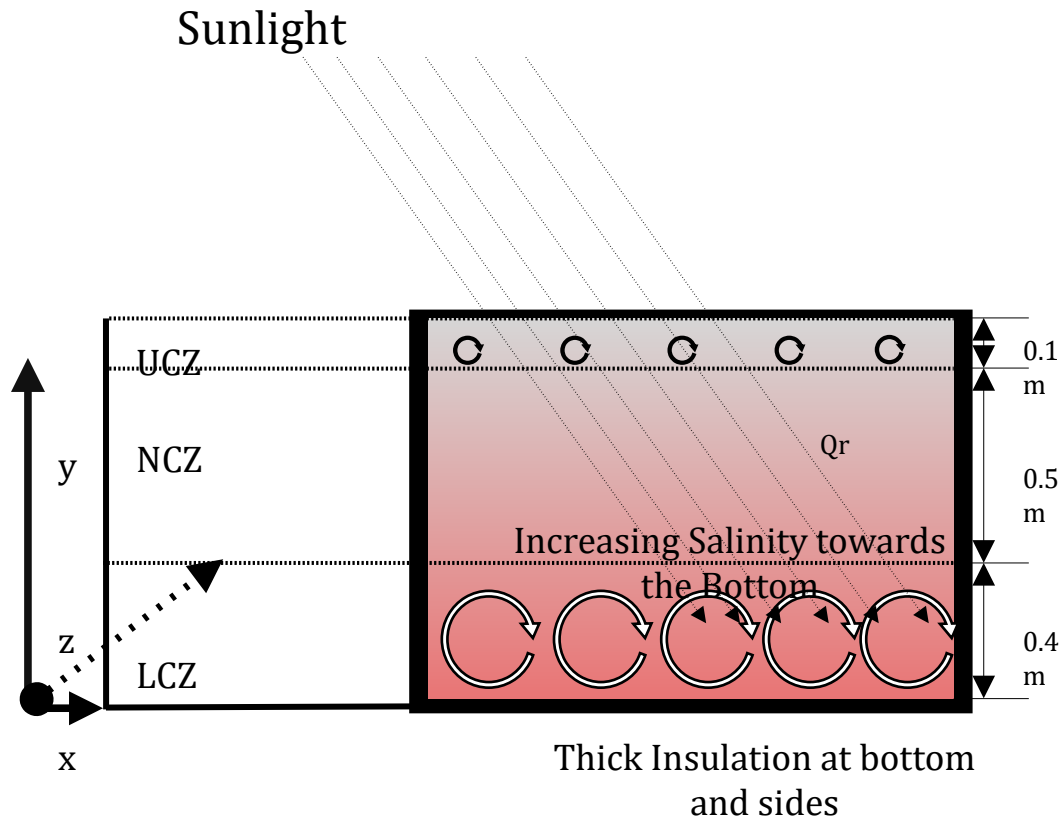


Figure 2. Schematic of Salt Gradient Solar Pond used to test the solver

- a) The velocity, temperature, and concentration variation along the z -direction is considered small enough so that it is negligible. Therefore, the velocity, temperature, and concentration distributions within the pond are two-dimensional.
- b) Both the vertical and the bottom walls of the pond are well insulated and impermeable.

- c) The incident solar radiation upon the free surface of the pond is a supposed constant and has an average value in transient regime as per Rabl and Nielsen (1975).
- d) The solar radiation that reaches the bottom of the pond is evaluated for the fluid at this depth as per Equation (15) and (16).
- e) The mixture of salt and water is assumed to be incompressible and Newtonian.

Finally, The fluid properties are assumed independent of temperature and salt concentration and the values used are mentioned in the Appendix. The only property which is allowed to have a variation is the density which varies according to the Boussinesq approximation as Equation (3)

The governing equations from (1) to (5) have been implemented in the solver, with the following Generalisations and consideration for the initial and boundary conditions:

3.4. Initial and boundary conditions:

For all the simulation runs, for Initial condition the water inside is at rest and at ambient temperature:

$$T=293K, \vec{V}=0\text{m/s and } p = 0$$

The initial salt concentration for different cases is distributed in the SGSP as follows:

- The LCZ has a salt concentration of 100mol/m^3 , 300mol/m^3 , 600mol/m^3 and 1000mol/m^3

- The salt concentration in the NCZ varies linearly from 100mol/m³, 300mol/m³, 600mol/m³ and 1000mol/m³ to 0mol/m³
- There is no salt in the UCZ
- Two type of Boundary Conditions have been tested for Salt concentration at the bottom, 1.) Fixed Boundary Condition & 2.) Zero Gradient Boundary Condition

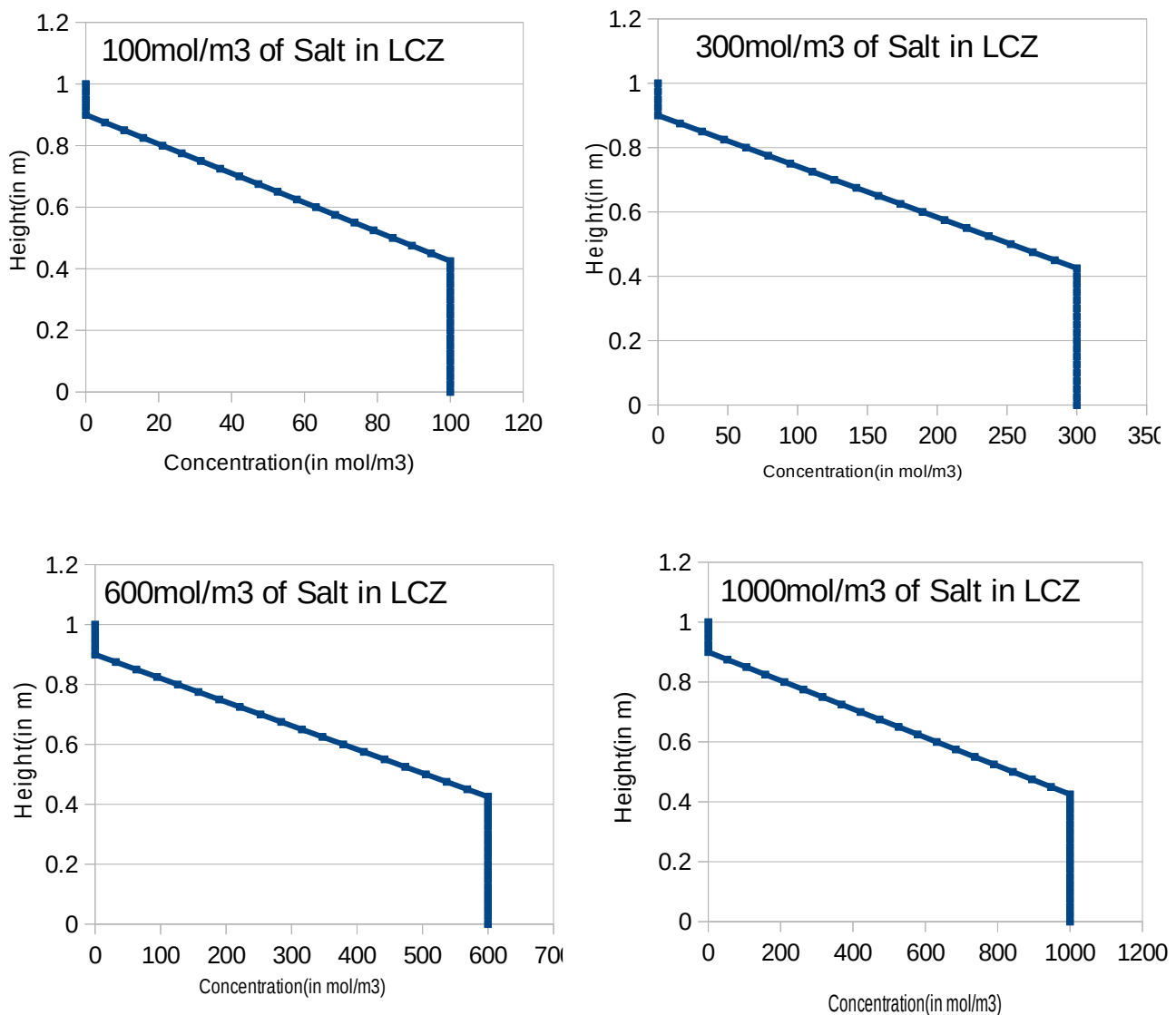


Figure 3. Initial Salt Concentration conditions.

With regard to the boundary conditions the vertical walls of the model pond is thermally insulated and impermeable, at the bottom there is zero mass flux and heat flux is same as radiation reaching the depth. At the surface the velocity boundary condition is zero.

Similarly, the heat flux available at a certain depth is evaluated as per Equation (15) and (16) and has been introduced as a source to the code, which is evaluated on the basis of three separate values of incident radiation of 250W/m², 500W/m² and 1000W/m² at the pond surface .

3.5. Courant Number:

The Courant number is non-dimensional number used in Computational Fluid Dynamics (CFD) simulations to evaluate time step requirements for a given mesh size and flow velocity. It is of paramount importance in transient simulations.

The formula for Courant number C_o is :

$$C_o = \frac{U \Delta t}{\Delta h} \text{-----(17)}$$

where,

U : Flow velocity

Δt : time step

Δh : characteristic size of the mesh cell

Similarly for Multidimensional flow, The courant number may be expressed as :

$$C_o = \sum_i \left(\frac{U \Delta t_i}{\Delta h_i} \right) \text{-----} (18)$$

this parameter provides an understanding about how much information propagates across a computational grid cell in a unit of time. A value greater than 1, indicates that a fluid particle and all its relevant information propagates through more than grid cell at a time and this leads to inaccurate and non-physical results. This also leads to divergence in solution.

The relation indicated by equations (17,18), hold an important bearing on the combinations of time-step and grid cell size in checking for grid convergence, and also on the entire development and execution of the solver as a whole.

For every step of the simulation, it **has been ensured to check on the Courant number to keep it below 1.**

3.6. Testing Grid Convergence:

To ensure that the solver is independent of the grid which has been utilised, five sets of combination of grid spacing length and time-step are used, a run time of 10 days has been utilised for all such combinations. Both temperature and concentration values at the interface of LCZ and NCZ has been investigated.

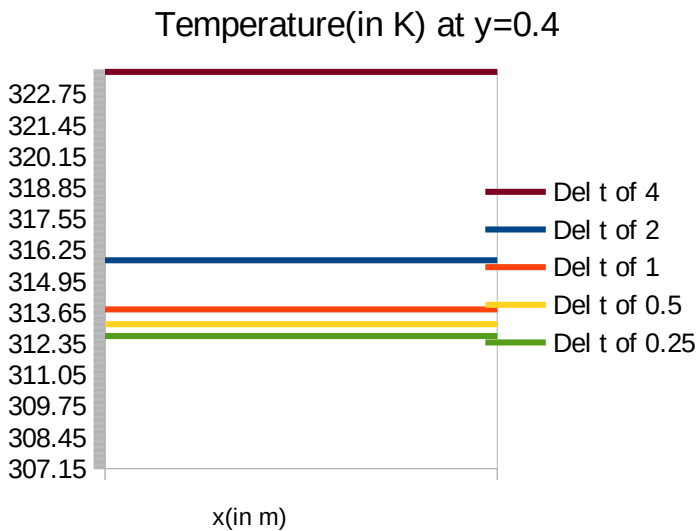


Figure 4(a). Grid convergence test with Temperature

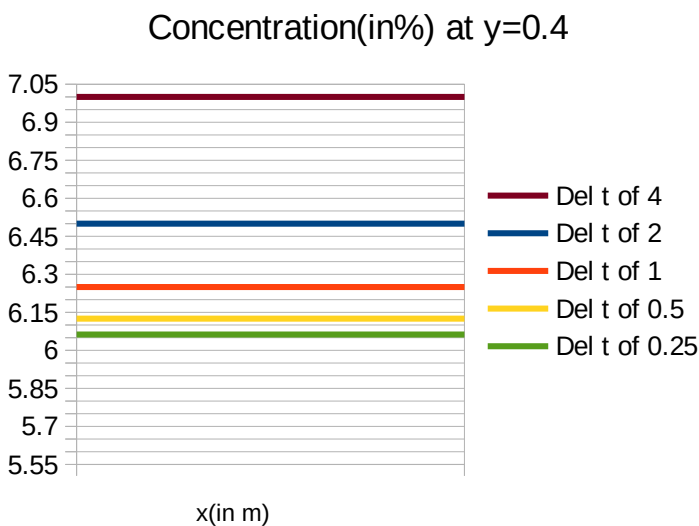


Figure 4(b). Grid convergence test with Concentration

From the above revelation a time step of 0.5 seconds and a Grid of 40x40 may be considered relatively suitable for the present work and the Grid may be considered independent.

4.Results and Discussion:

4.1.Validation of the Solver:

With the time step and Grid separation length decided the solver is then validated against experimental studies on SGSP in past publications where the code is adjusted to incorporate the input data as provided by the same.

1. The following comparison has been established with data from M.R. Jaefarzadeh , 2004[27]. The radiative heat flux has been obtained from the paper itself while the radiation at depth is evaluated using the Correlation provided by Rabl and Nielsen, 1975[25]. The availability of sunlight hours is evaluated using equations (7),(9) and (10); and the latitude data of the location of the Experiment. Initial conditions have been obtained from M.R. Jaefarzadeh , 2004[27], for initial temperature, and heat loss which has been directly provided in M.R. Jaefarzadeh , 2004[27] .

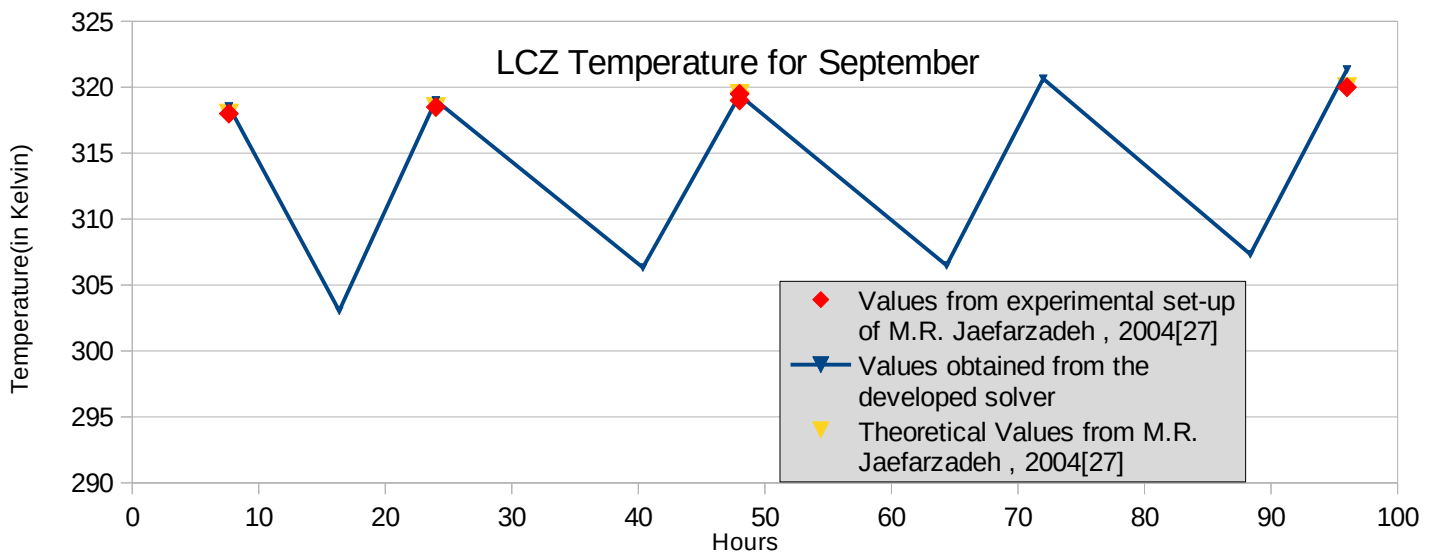


Figure 5(a). Temporal evolution of average LCZ Temperature for the month of September and comparison with experimental and theoretical values of M.R. Jaefarzadeh , 2004[27]

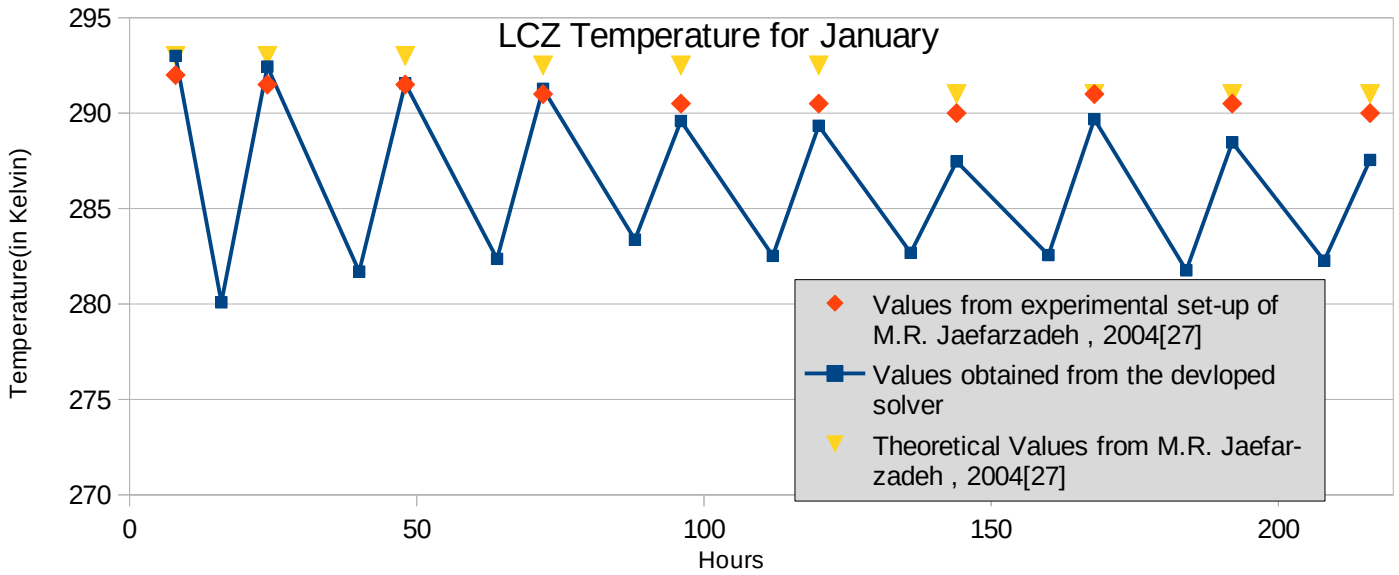


Figure 5(b). Temporal evolution of average LCZ Temperature for the month of January and comparison with experimental and theoretical values of M.R. Jaefarzadeh , 2004[27]

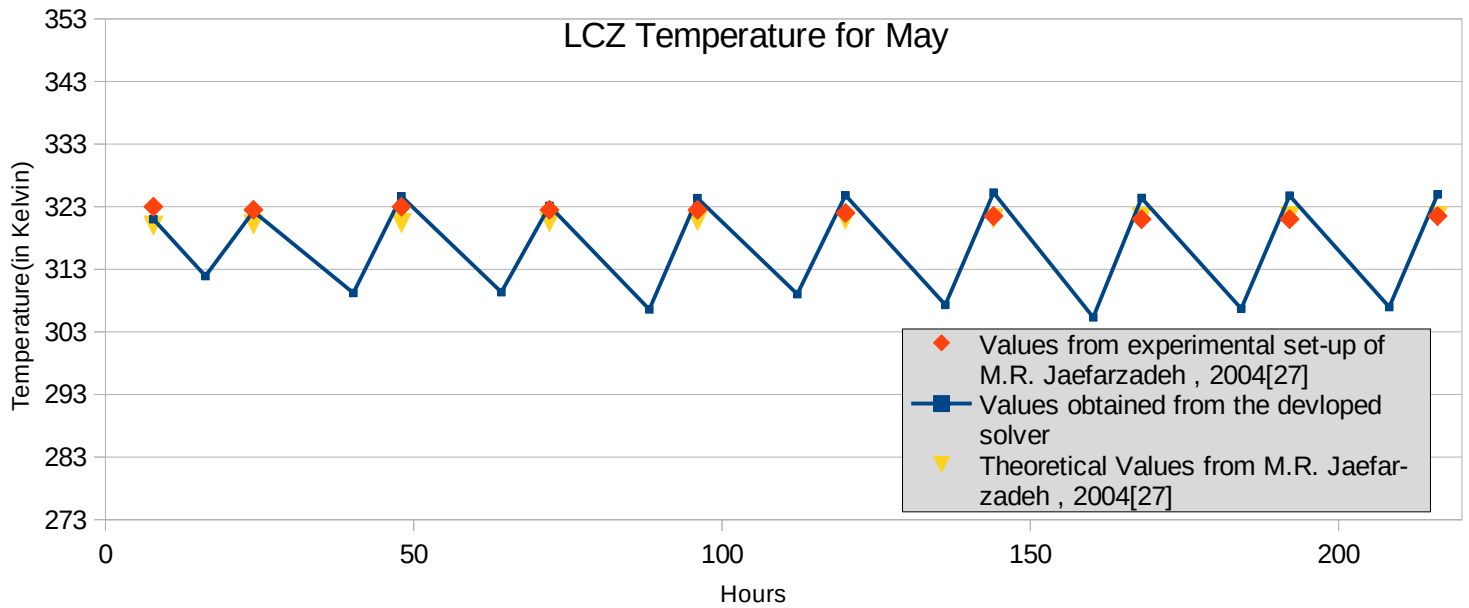


Figure 5(c). Temporal evolution of average LCZ Temperature for the month of May and comparison with experimental and theoretical values of M.R. Jaefarzadeh , 2004[27]

It is to be noted that the zones of depression, or rather a reduction in the temperature of the LCZ is due to the loss of heat during hours without sunlight and the loss value is used directly as shown in M.R. Jaefarzadeh , 2004[27] . The Solvers performance during this comparison has yielded satisfactory results.

2. The solver is further tested against the experimental findings form Dah, Mohamed El Mokhtar & Ouni, M. & Guizani, A. & Belghith, Abdelfettah. (2004) [30]. The concentration boundary condition at the bottom is 15wt% and the Incident radiation Data has been given as 1000W/m^2 . Heat loss from surface is taken as 5W/m^2 . The Initial Temperature of the pond is 296K. The radiation heat flux available at the depth is obtained by the correlation provided by Rabl and Nielsen, 1975[25].

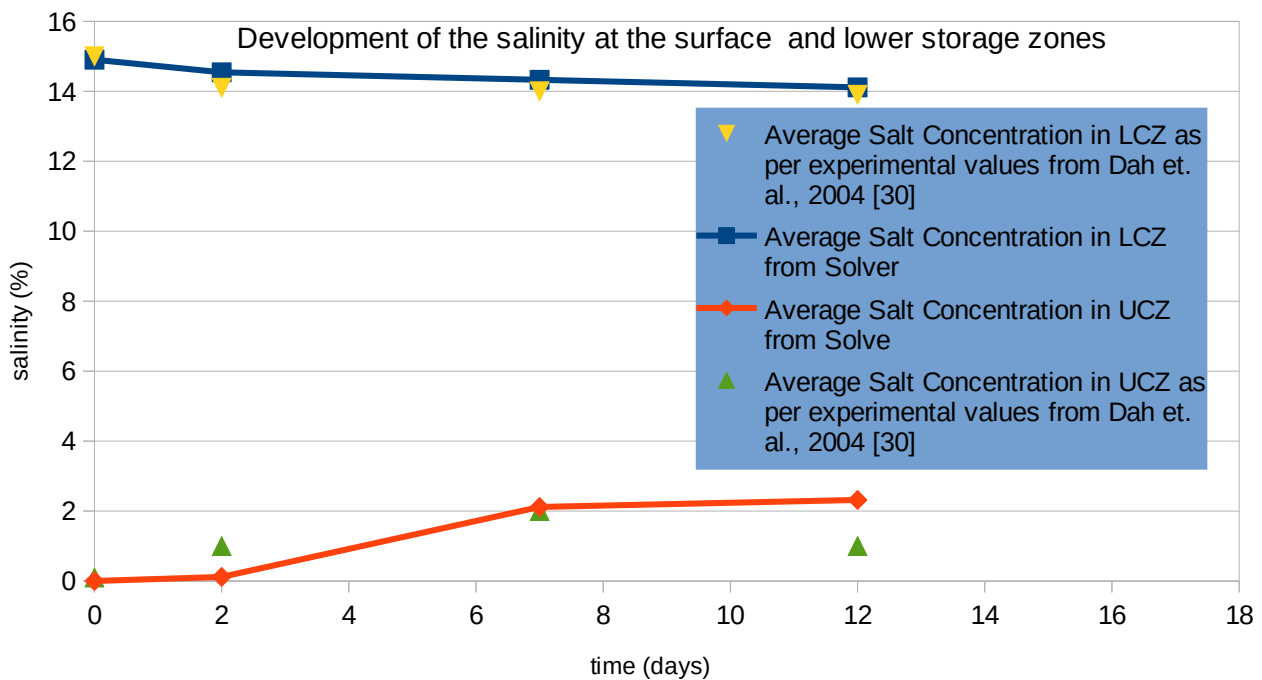


Figure 6(a). Temporal evolution of average LCZ and UCZ Concentration and comparison against experimental values from Dah et. al., 2004 [30]

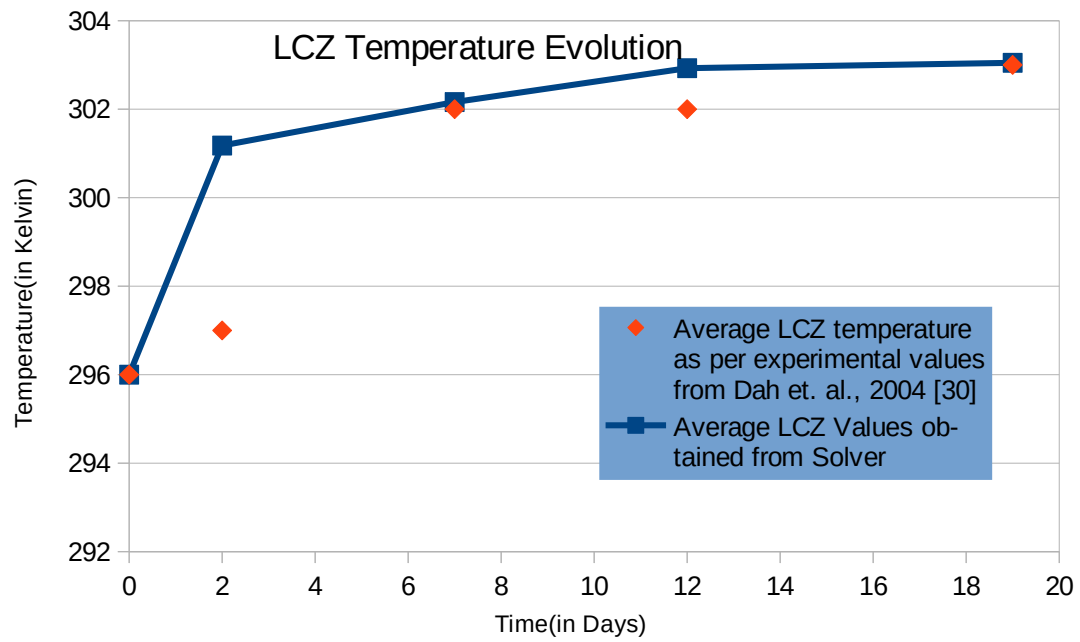


Figure 6(b). Temporal evolution of average LCZ and UCZ Temperature and comparison against experimental values from Dah et. al., 2004 [30]

4.2. Temporal Evolution of Temperature With varying values of Incident Radiation where initial temperature of the pond is 293K and the walls and bottom of the pond have zero gradient boundary condition for temperature:

4.2.(a).For Radiation Value of 250W/m^2 and loss of 4W/m^2 from the surface:

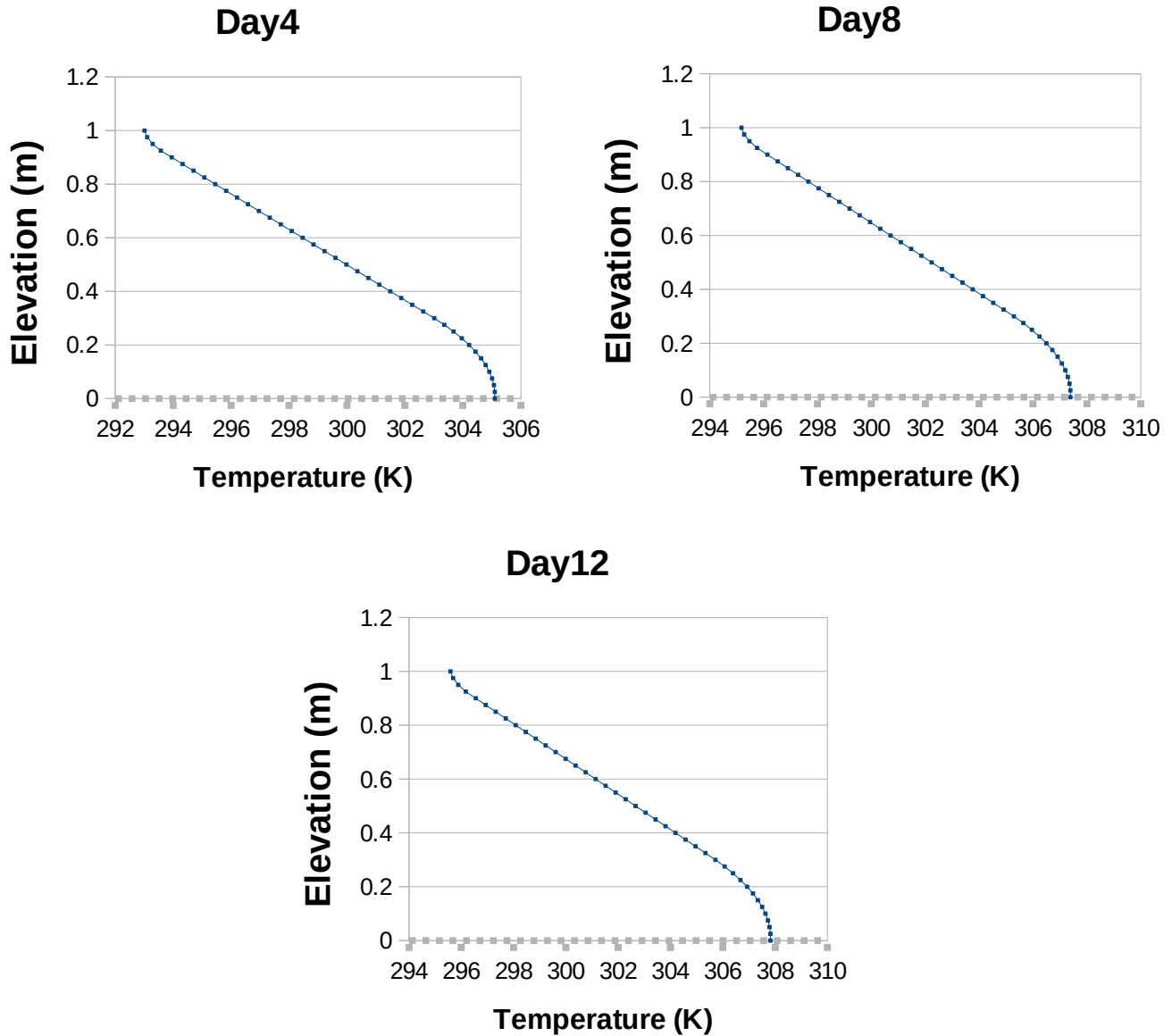


Figure 7(a). Temperature v/s Elevation for Incident Radiation of 250W/m^2 .

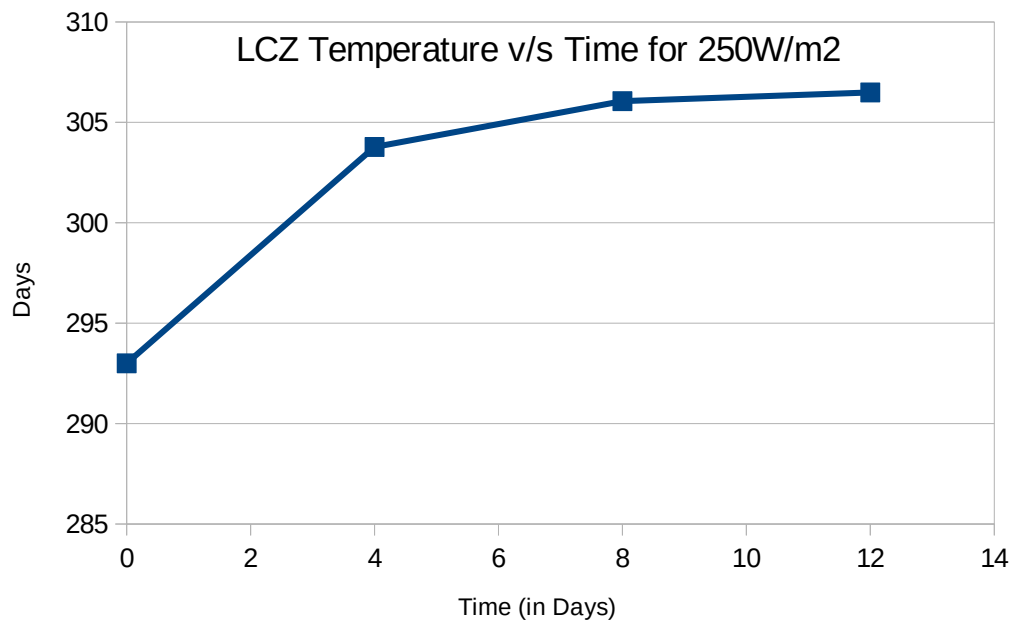


Figure 7(b). Average LCZ temperature v/s Time for Incident Radiation of 250W/m².

4.2.(b). For Radiation Value of 500W/m² and loss of 4W/m² from the surface:

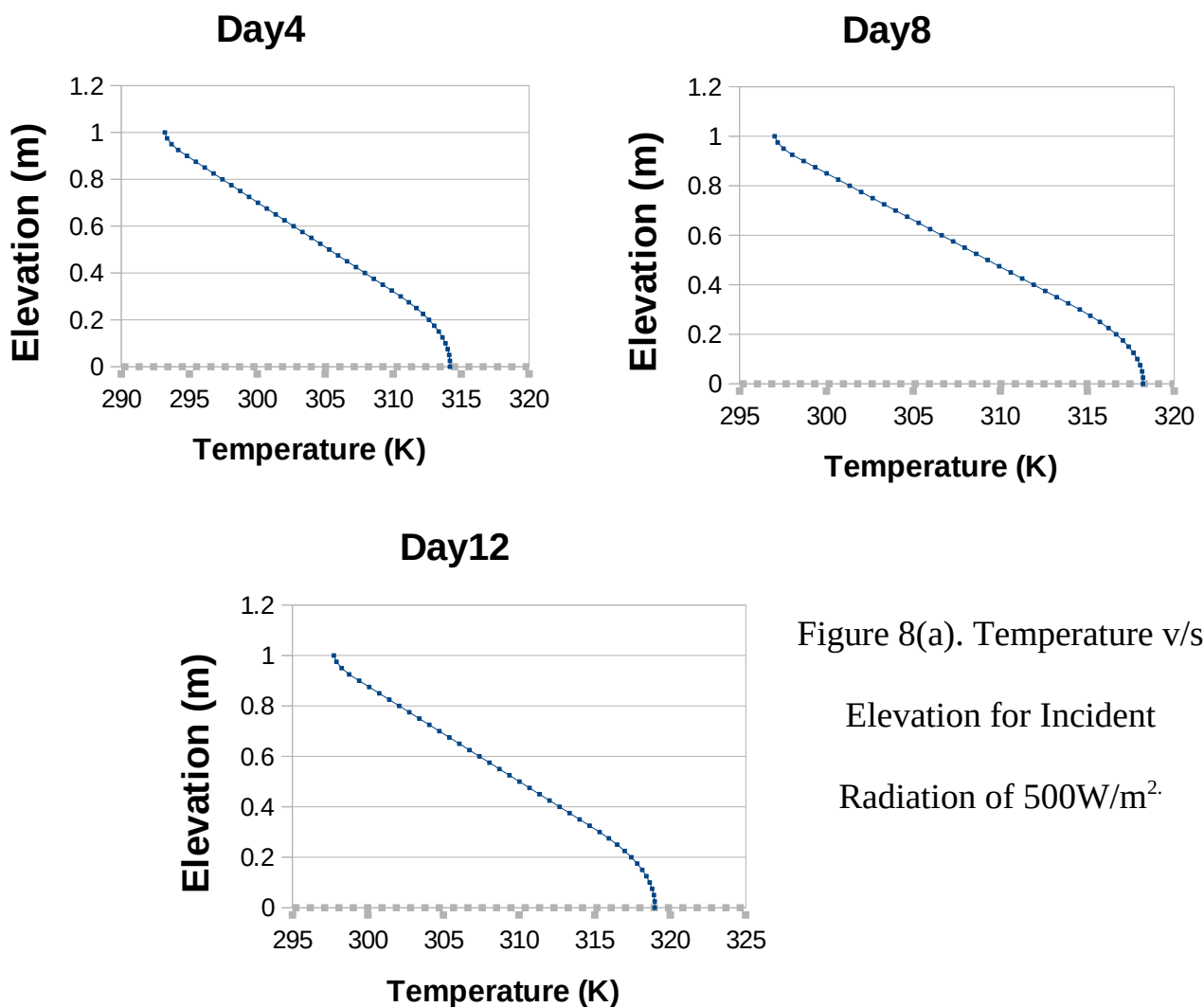


Figure 8(a). Temperature v/s
Elevation for Incident
Radiation of 500W/m².

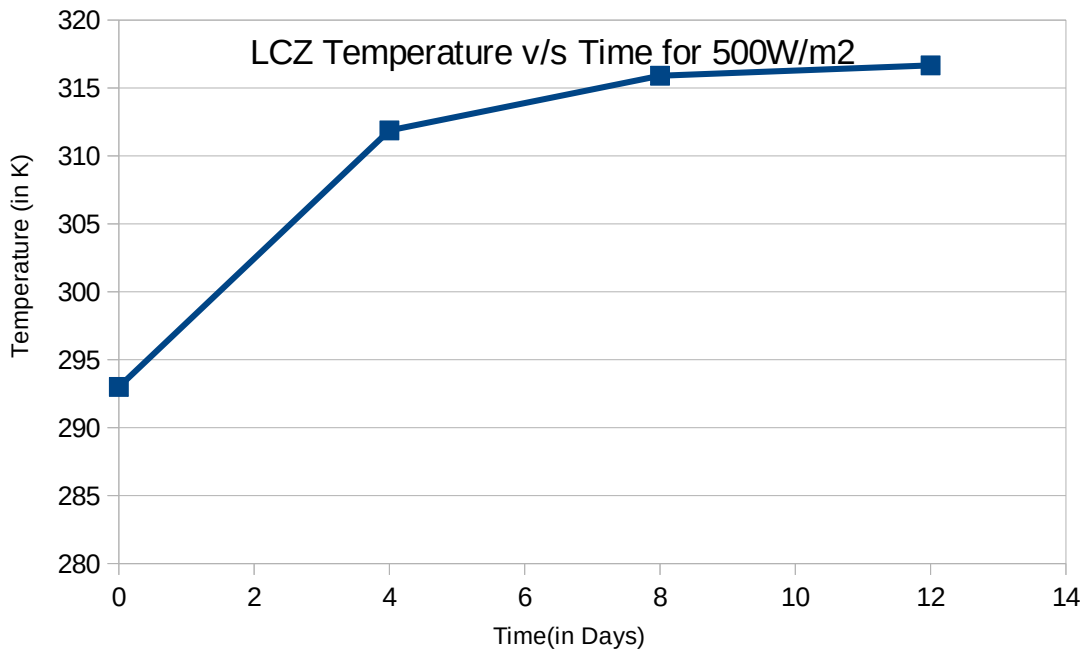


Figure 8(b). Average LCZ temperature v/s time for Incident Radiation of 500W/m².

4.2.(c). For Radiation Value of 1000W/m² and loss of 4W/m² :

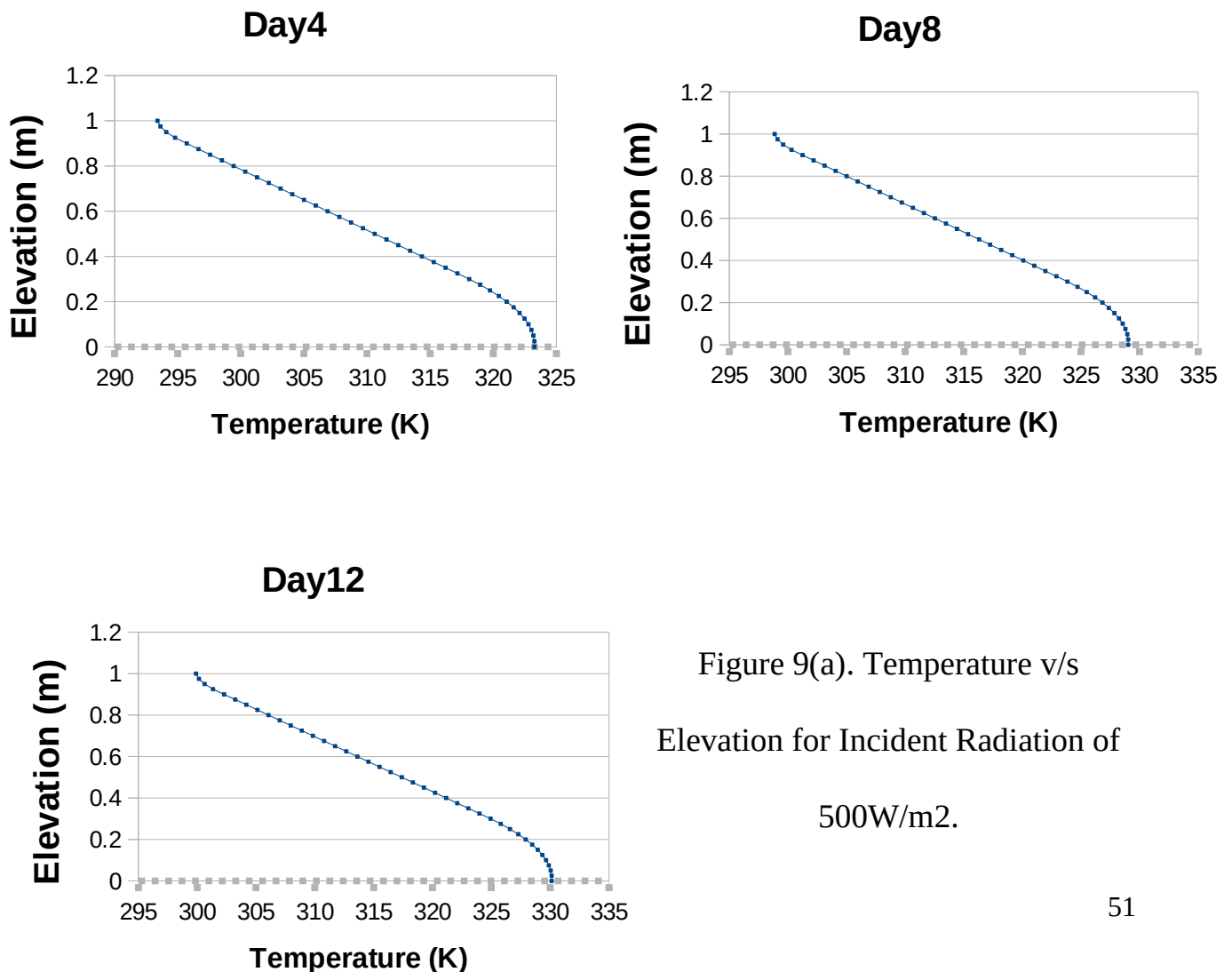


Figure 9(a). Temperature v/s Elevation for Incident Radiation of 500W/m².

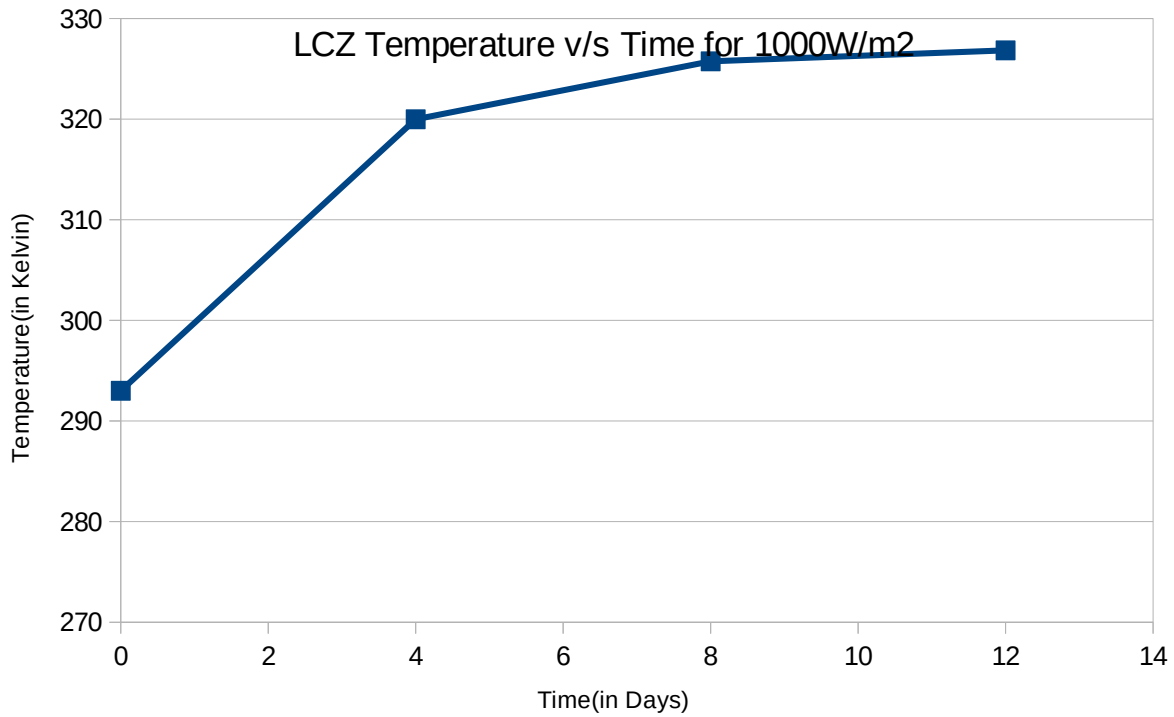


Figure 9(b). Average LCZ temperature for Incident Radiation of 1000W/m².

As as per the temporal evolution curves obtained from the various values of incident radiation it is clearly visible that linear profiles for temperature is obtained in the non convection zone while temperature remains without a gradient in the upper and lower convection zone. It is also seen that with the increase in the value of the incident radiation the temperature gains in the lower convection zone increases. This behaviour is similar to an actual salt gradient solar pond. The temperature will not continue to increase indefinitely leading to extreme temperatures in the LCZ as a loss value has been incorporated at the surface as per M.R. Jaefarzadeh , 2004[27]. The upper convection zone which remains in constant contact with the surrounding atmosphere for an actual SGSP, has a relatively small change introduce to it as it loses heat constantly to the ambient, this behaviour for the model pond is established by incorporating a heat loss component directly into the solver.

4.3.(a) Comparison and discussion for Change in Temperature profile with varying amount of incident radiation:

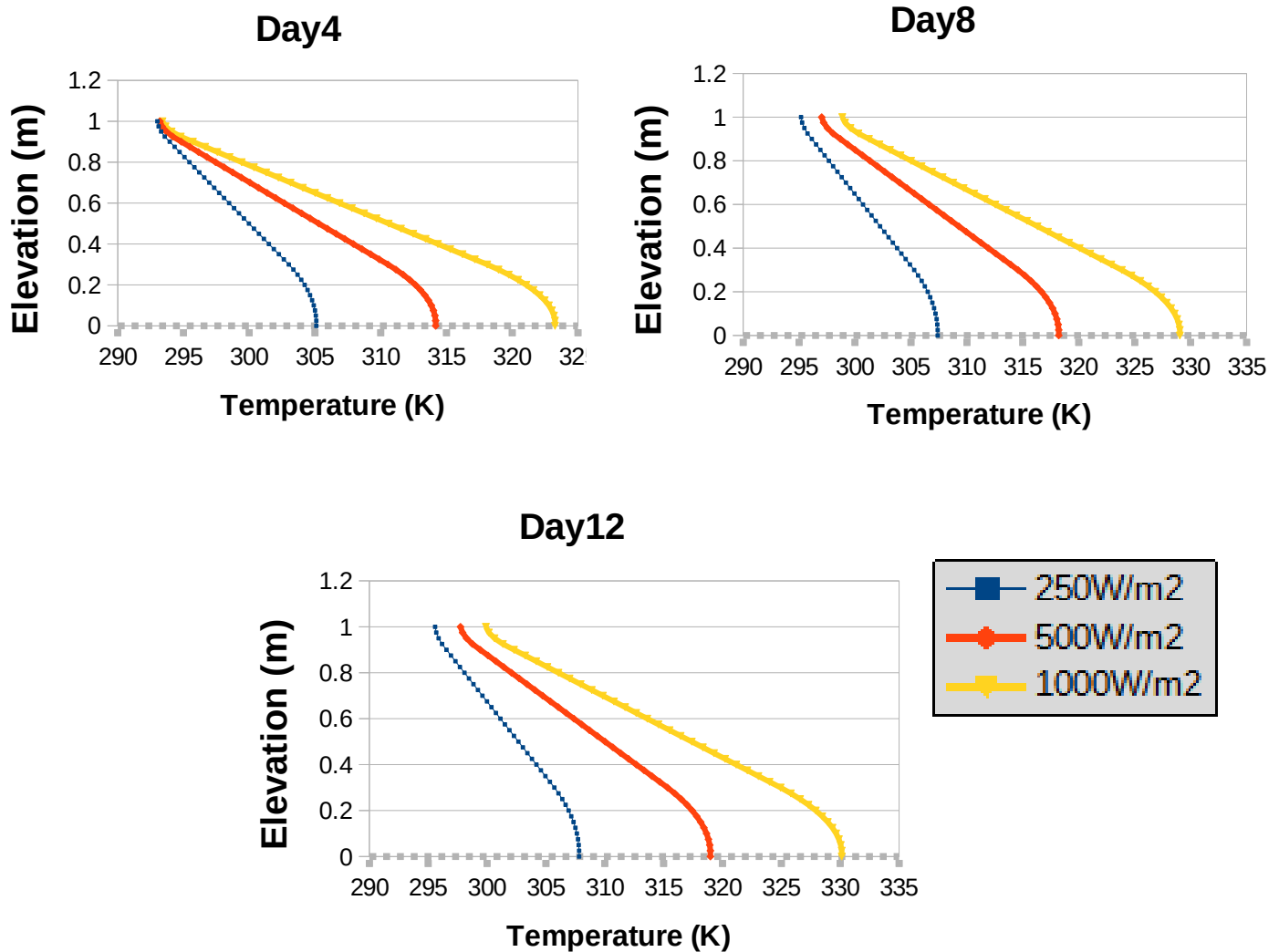


Figure 10(a). Temperature profiles of pond developed over time with varying values of incident Radiation.

With increase in Incident radiation, the heat energy absorbed by the pond increases, this gain in energy and subsequent rise in temperature of the solar pond. A linear profile of temperature with height is observed in the NCZ while the LCZ and UCZ have almost no gradient, which indicates mixing of temperature in the LCZ and UCZ.

As, the value of incident radiation inscreases, the gradient established across the height of the Solar Pond becomes steeper. Also, the gradient becomes steeper, with the passage of time.

4.3.(b). Comparison and discussion for Change in Average LCZ temperature over time with varying amount of incident radiation:

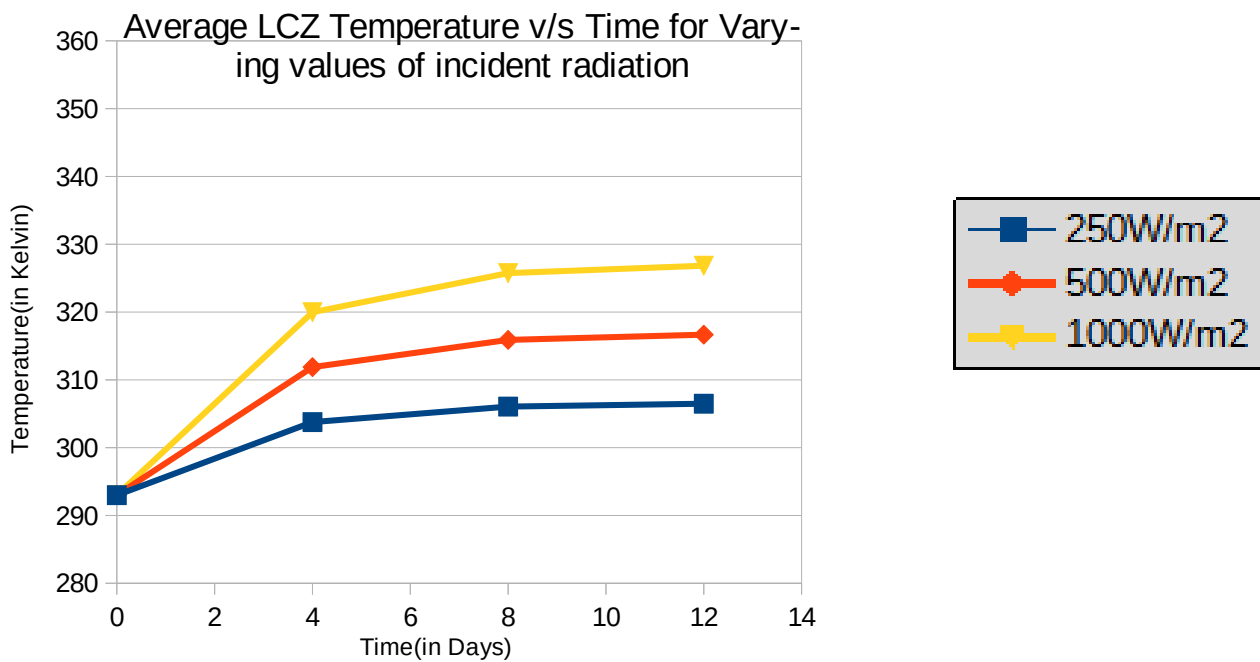


Figure 10(b). Average LCZ temperature over time with varying amount of incident radiation.

In the LCZ the average temperature starts to gradually increase with time for all values of incident radiation, with higher average temperature observed in the LCZ for higher Radiation value. However, the value of avearge temperature starts to stabillise after a period of 10 days, as seen in figure 10.(b), this is due to the constant loss of energy from the model pond which causes it to reach a steady state.

4.4. Temporal Evolution of Concentration With varying values of Salt Concentration and different Boundary Condition in LCZ (Incident Radiation value of 1000W/m^2) :

4.4.i. Zero Gradient Condition for Salt Concentration at bottom Boundary.

4.4.i.(a) 100mol/m^3 salt concentration in LCZ with zero gradient condition at the bottom boundary

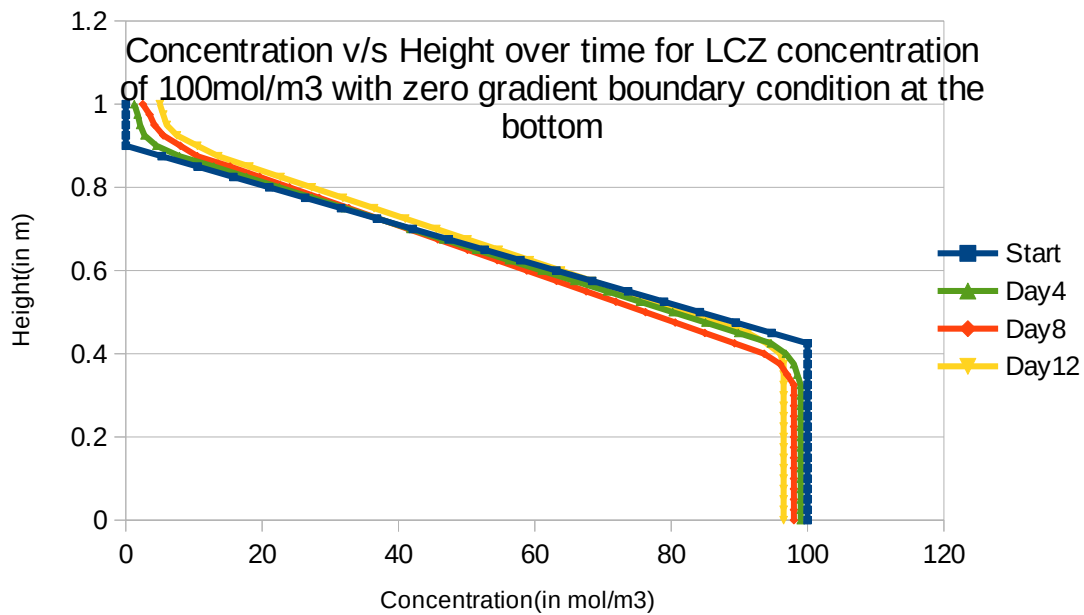


Figure 11(a). Concentration v/s Height over time for 100mol/m^3 salt concentration in LCZ with zero gradient condition at the bottom boundary

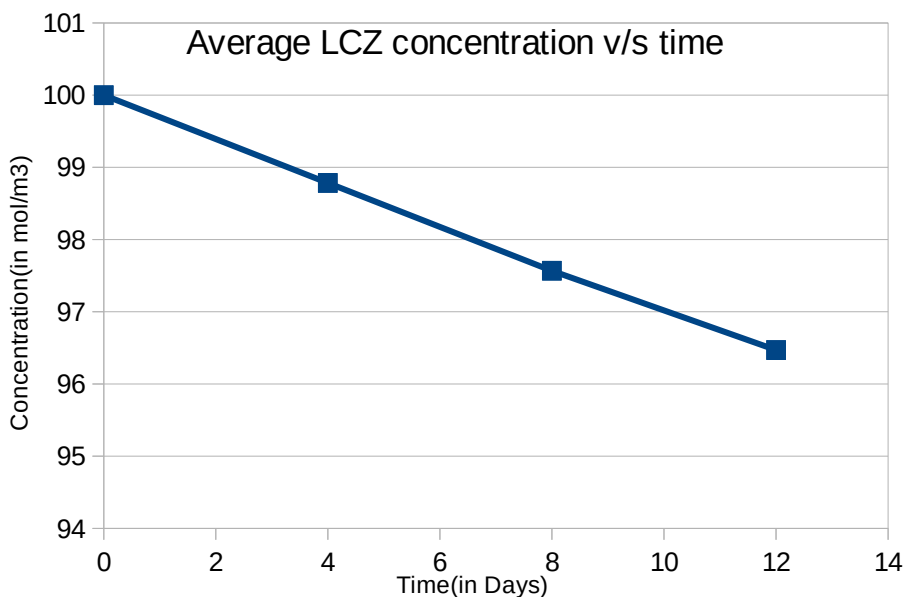


Figure 11(b). Average LCZ Concentration v/s time for 100mol/m^3 salt concentration in LCZ with zero gradient condition at the bottom boundary

4.4.i.(b) 300mol/m³ salt concentration in LCZ with zero gradient condition at the bottom boundary

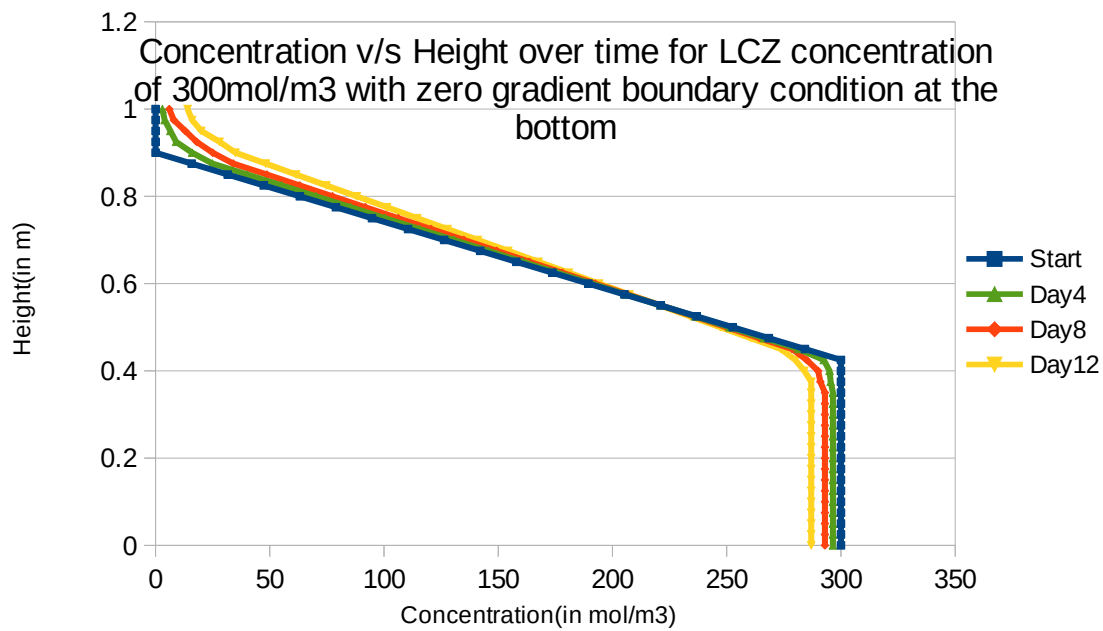


Figure 12(a). Concentration v/s Height over time for 300mol/m³ salt concentration in LCZ with zero gradient condition at the bottom boundary

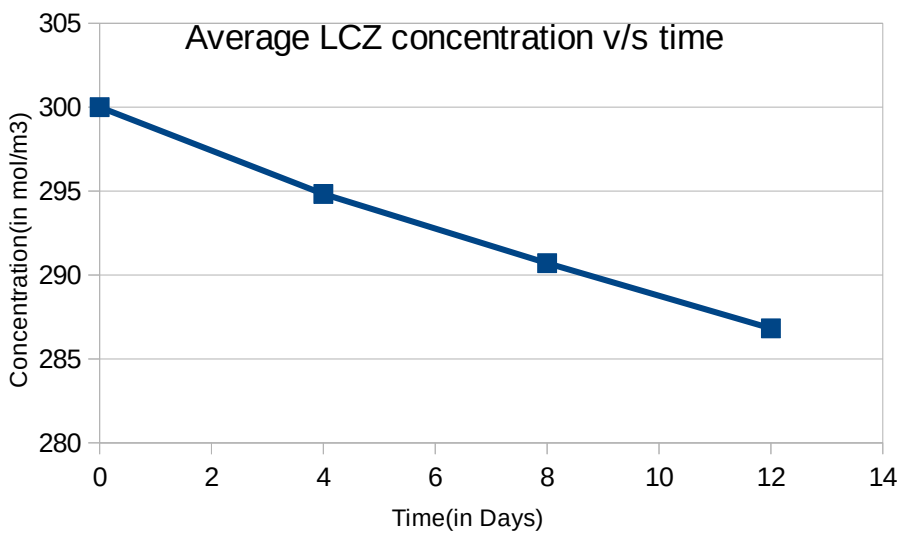


Figure 12(b). Average LCZ Concentration v/s time for 300mol/m³ salt concentration in LCZ with zero gradient condition at the bottom boundary

4.4.i.(c) 600mol/m³ salt concentration in LCZ with zero gradient condition at the bottom boundary

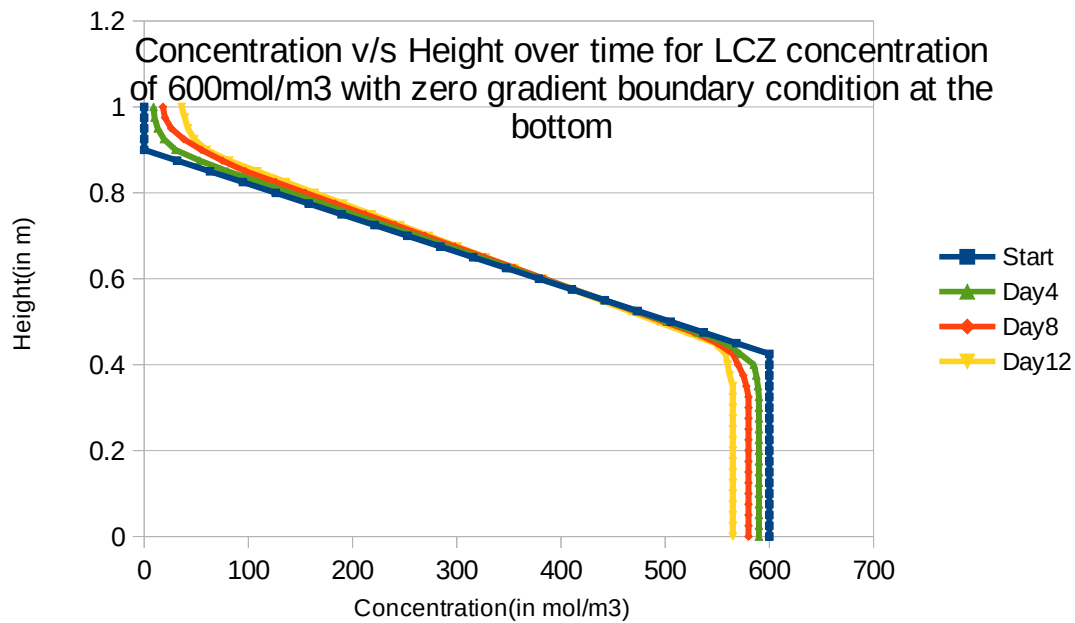


Figure 13(a). Concentration v/s Height over time for 600mol/m³ salt concentration in LCZ with zero gradient condition at the bottom boundary

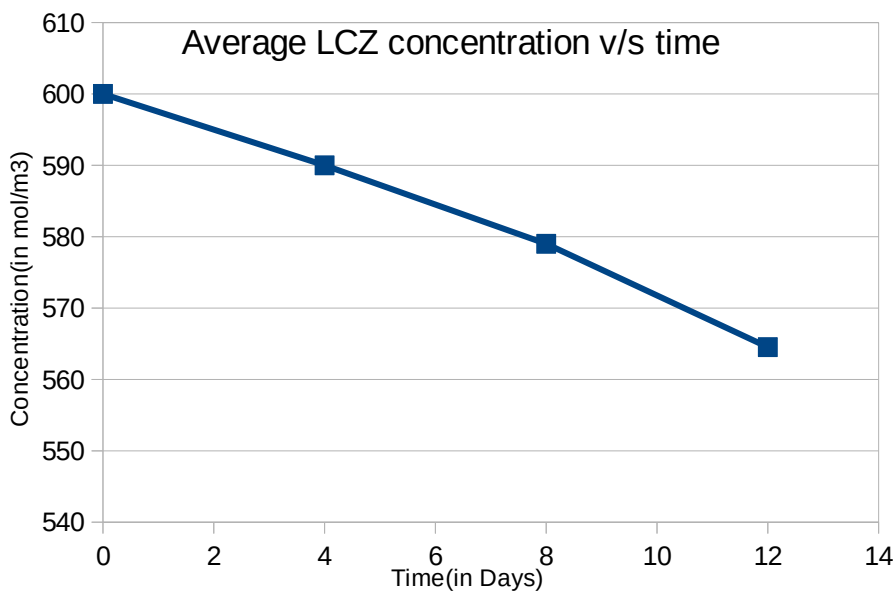


Figure 13(b). Average LCZ Concentration v/s time for 300mol/m³ salt concentration in LCZ with zero gradient condition at the bottom boundary

4.4.i.(d) 1000mol/m³ salt concentration in LCZ with zero gradient condition at the bottom boundary

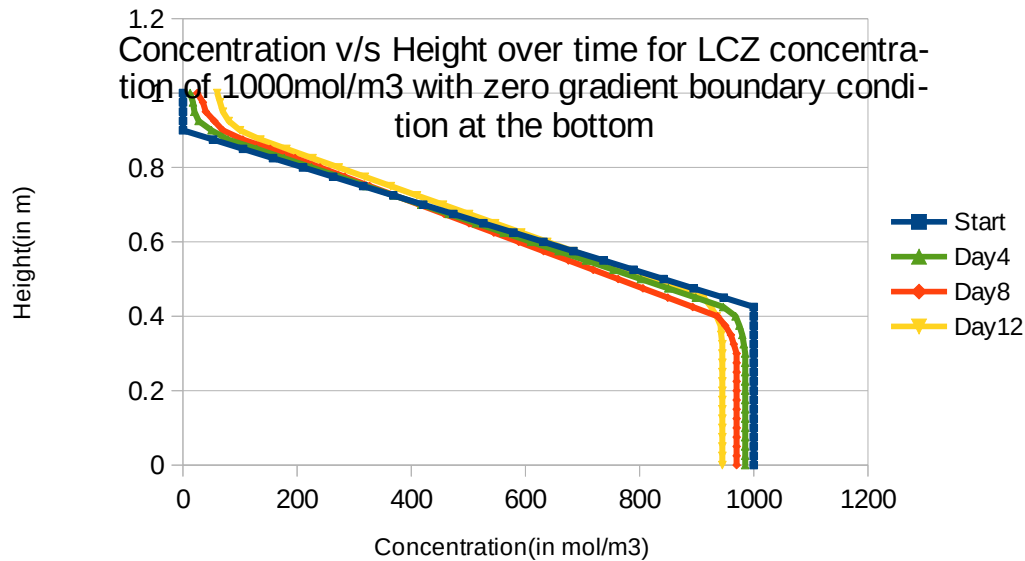


Figure 14(a). Concentration v/s Height over time for 1000mol/m³ salt concentration in LCZ with zero gradient condition at the bottom boundary

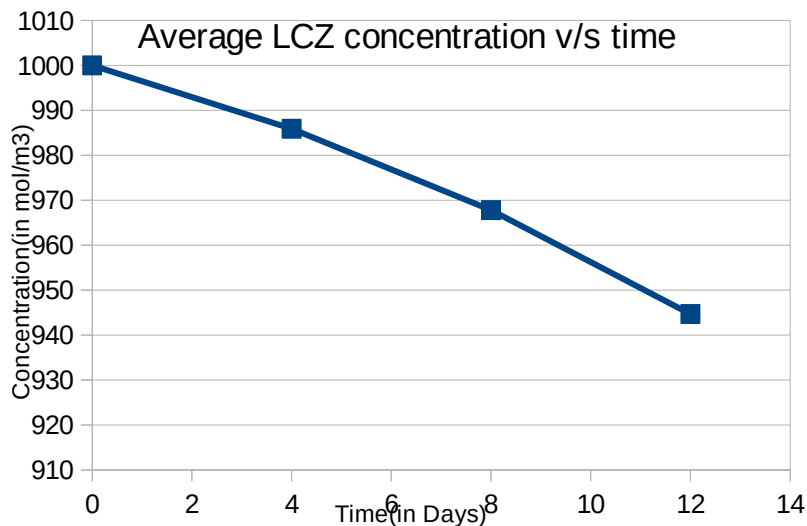


Figure 14(b). Average LCZ Concentration v/s time for 1000mol/m³ salt concentration in LCZ with zero gradient condition at the bottom boundary

With passage of time, salt concentration in the LCZ gradually reduces with a subsequent increase of salt concentration in the UCZ, with the highest salt

concentration accumulating in the UCZ for the case with 1000mol/m^3 salt concentration in the LCZ initially as seen from figure 11(a), 12(a), 13(a) and 14(a). This happens due to diffusion of salt from the LCZ. As, this diffusion of salt occurs the salt gradient which has been established initially, gradually becomes less steep over time. This reduction in steepness of the salt gradient which occurs over time becomes more pronounced with increased Initial salt concentration in the LCZ, with the highest reduction in concentration gradient occurring for Initial salt concentration of 1000mol/m^3 and least for initial salt concentration of 100mol/m^3 . With zero-gradient boundary condition for concentration at the bottom boundary, the concentration profile observed in the LCZ , indicates that the concentration remains same throughout the LCZ for all cases of initial LCZ salt concentration when a zero-gradient boundary condition for concentration is used at the bottom boundary.

There is a reduction of average LCZ salt concentration over time as observed from figure 11(b), 12(b), 13(b) and 14(b). This reduction is due to diffusion of salt out of LCZ. The reduction of average concentration of salt in the LCZ over time, increases with increased initial salt concentration in the LCZ.

4.4.ii. Fixed concentration condition for salt at the bottom boundary

4.4.ii.(a) 100mol/m³ salt concentration in LCZ with fixed concentration condition at the bottom boundary

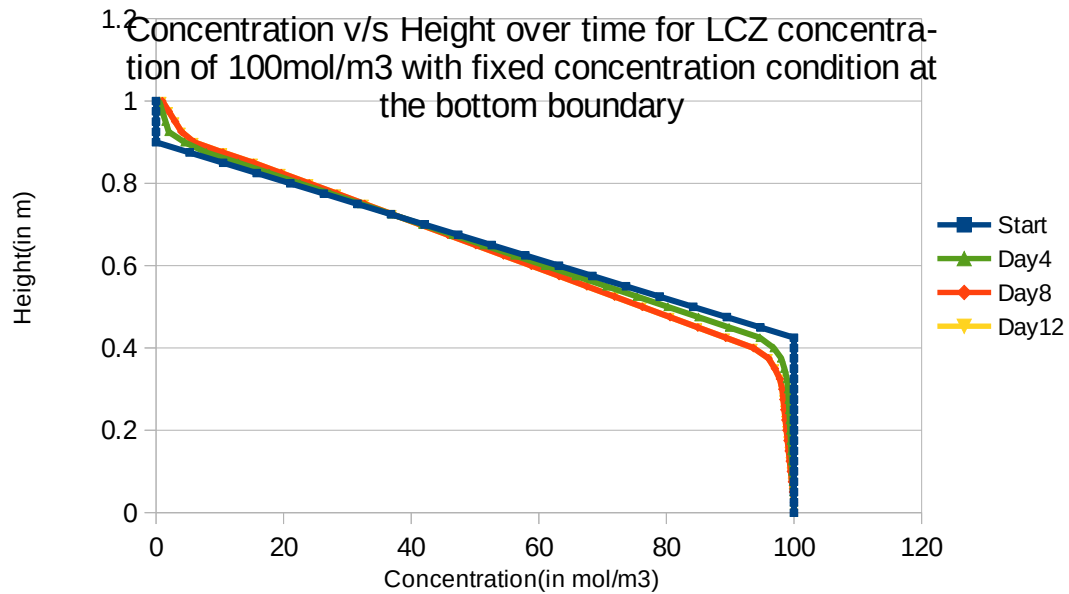


Figure 15(a). Concentration v/s Height over time for 100mol/m³ salt concentration in LCZ with fixed concentration condition at the bottom boundary

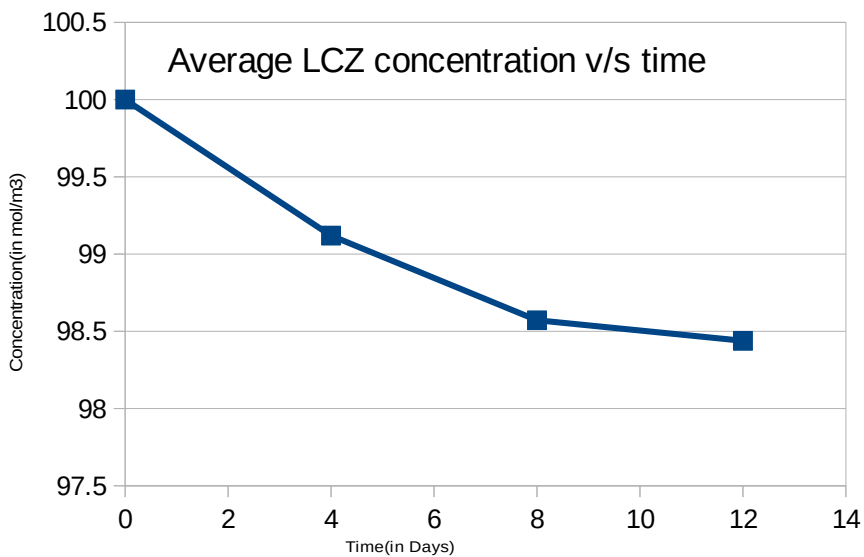


Figure 15(b). Average LCZ Concentration v/s time for 100mol/m³ salt concentration in LCZ with fixed concentration condition at the bottom boundary

4.4.ii.(b) 300mol/m³ salt concentration in LCZ with fixed concentration condition at the bottom boundary

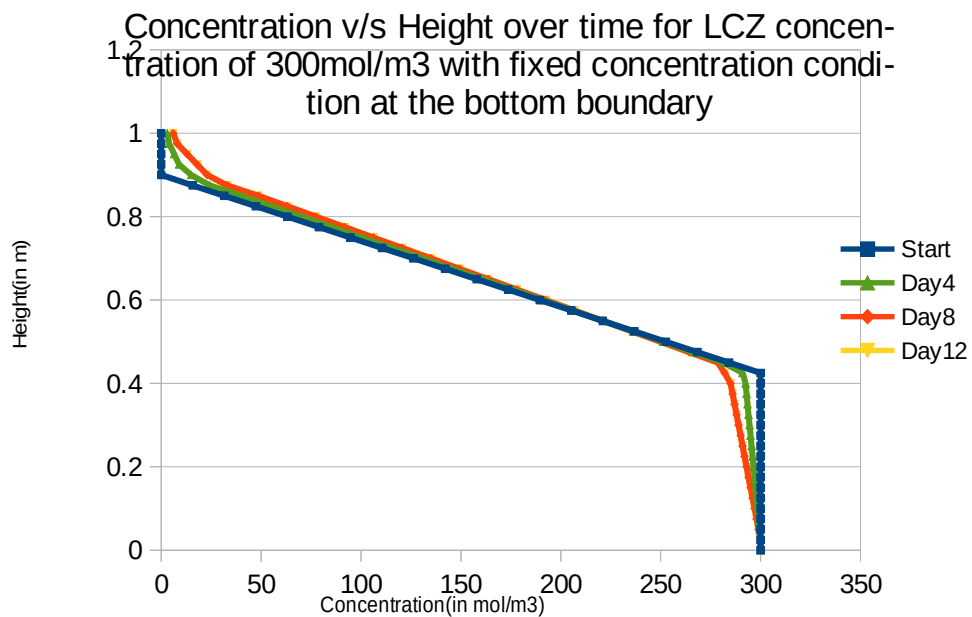


Figure 16(a). Concentration v/s Height over time for 300mol/m³ salt concentration in LCZ with fixed concentration condition at the bottom boundary

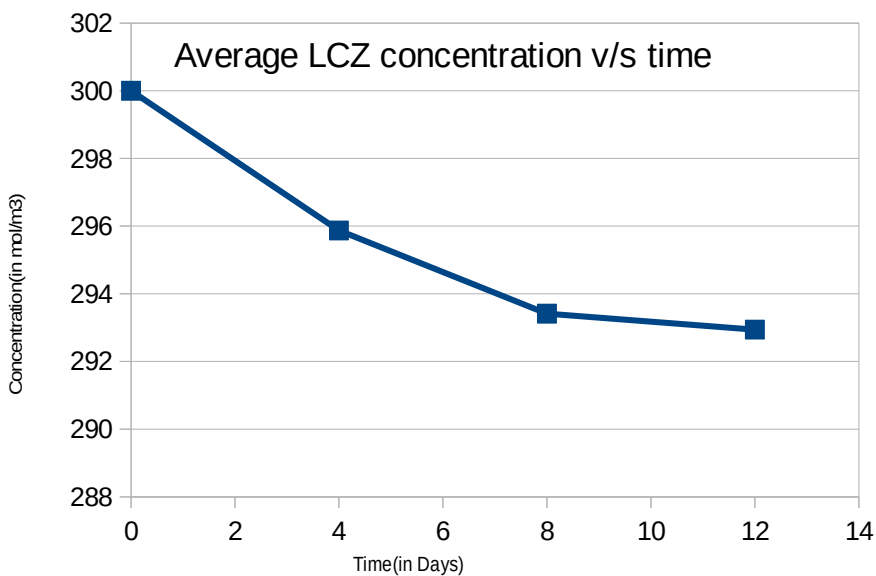


Figure 16(b). Average LCZ Concentration v/s time for 300mol/m³ salt concentration in LCZ with fixed concentration condition at the bottom boundary

4.4.ii.(c) 600mol/m³ salt concentration in LCZ with fixed concentration condition at the bottom boundary

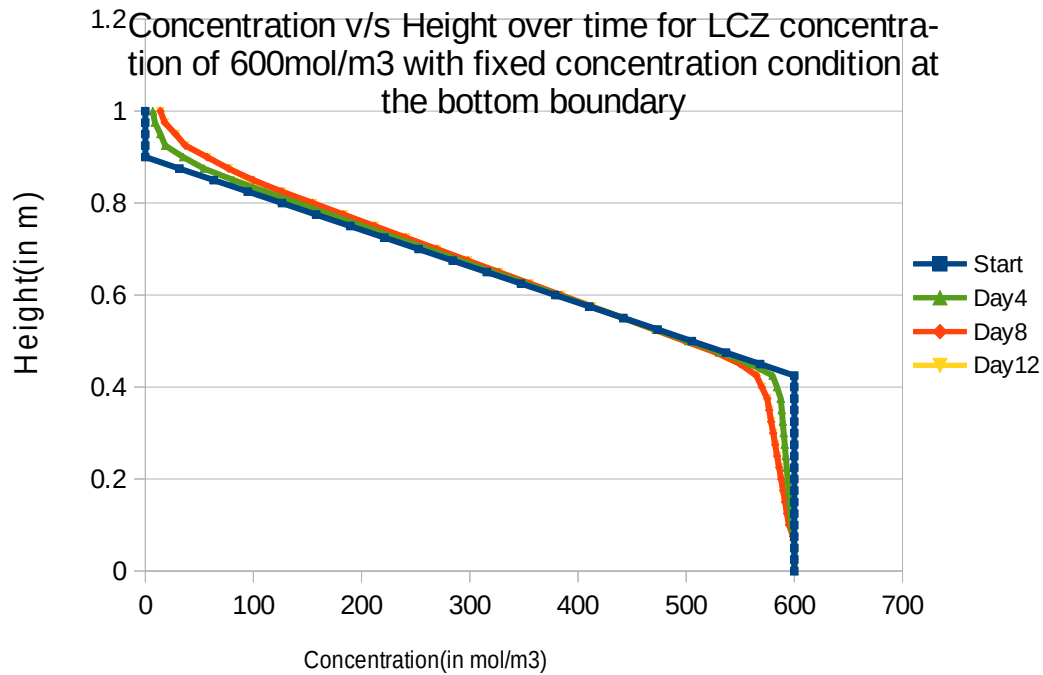


Figure 17(a). Concentration v/s Height over time for 600mol/m³ salt concentration in LCZ with fixed concentration condition at the bottom boundary

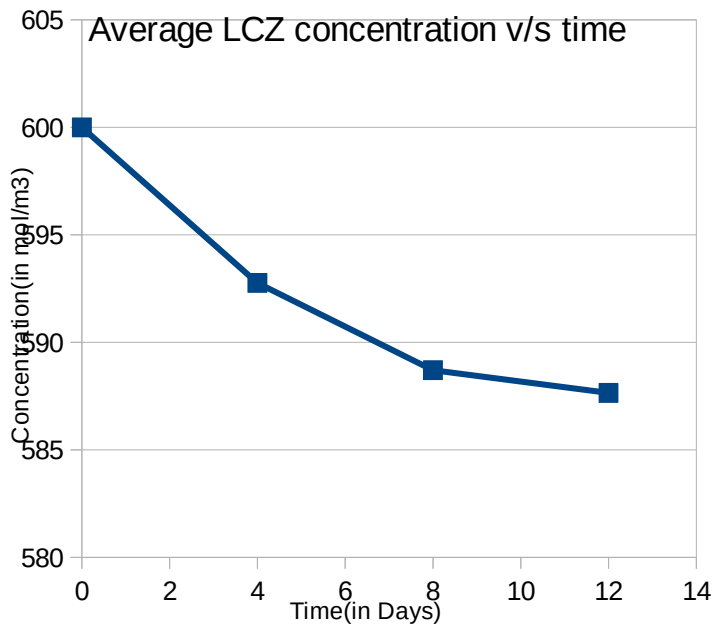


Figure 17(b). Average LCZ Concentration v/s time for 600mol/m³ salt concentration in LCZ with fixed concentration condition at the bottom boundary

4.4.ii.(d) 1000mol/m³ salt concentration in LCZ with fixed concentration condition at the bottom boundary

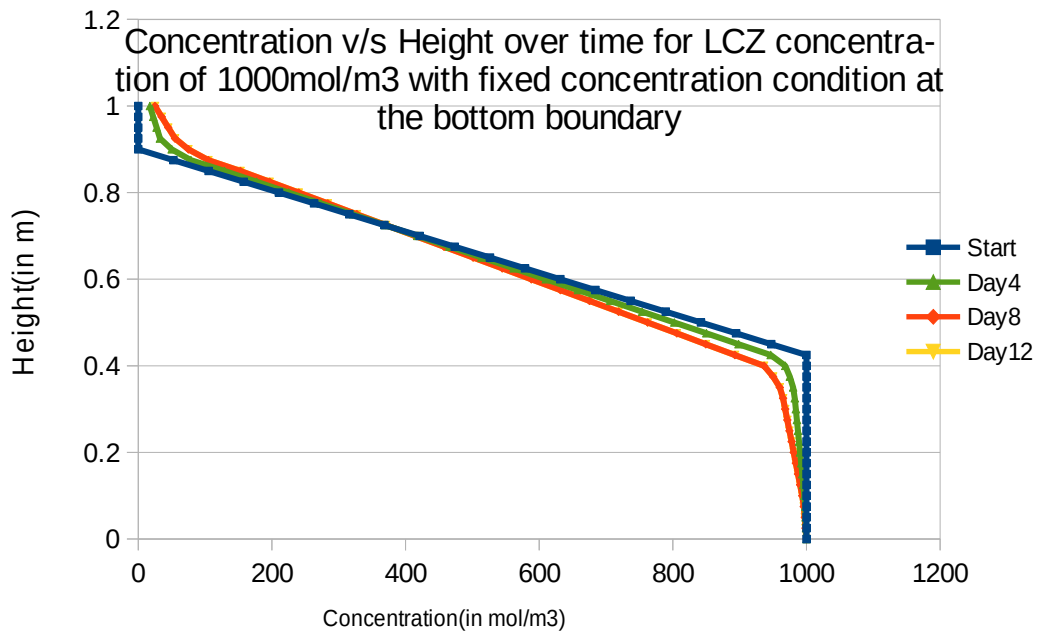


Figure 18(a). Concentration v/s Height over time for 1000mol/m³ salt concentration in LCZ with fixed concentration condition at the bottom boundary

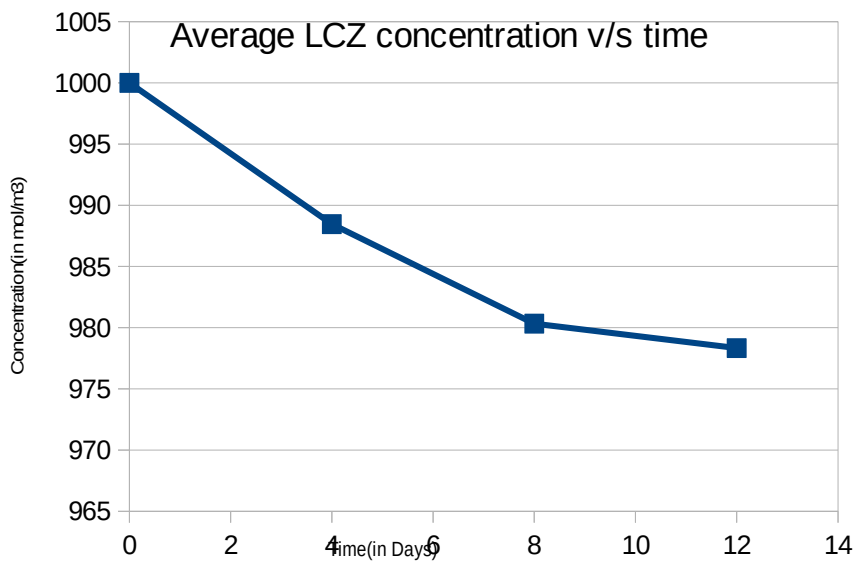


Figure 18(b). Average LCZ Concentration v/s time for 1000mol/m³ salt concentration in LCZ with fixed concentration condition at the bottom boundary.

In cases of fixed salt concentration condition in the bottom boundary, the profiles observed in figure 15(a), 16(a), 17(a) and 18(a), the salt concentration in the bottom layer and layers immediately in the vicinity, continue to stay at the value of the initial value of salt concentration, and the subsequent extent of reduction and increase in the respective values of concentration in LCZ and UCZ due to diffusion of salt is low. The concentration of Salt does not remain the same through the entire LCZ over time, as slight reduction of salt concentration occurs near the interface. The extent of reduction increases with increasing initial salt concentration in the LCZ.

The average salt concentration in the LCZ reduces with time figures 15(b), 16(b), 17(b) and 18(b) with highest reduction observed for initial salt concentration of 1000mol/m^3 , figure 18(b), and least reduction for 100mol/m^3 , figure 15(b), however the diffusion of salt out of LCZ for all cases of initial salt concentration of 100mol/m^3 , 300mol/m^3 , 600mol/m^3 and 1000mol/m^3 in the LCZ with fixed concentration condition at the bottom boundary slows down as the curves tend to flatten out and the reduction of average salt concentration in the LCZ with time in case of fixed salt concentration condition in the bottom boundary is much less than for cases with zero-gradient boundary condition for concentration at the bottom boundary.

4.5. Comparison for Change in Concentration Profile and average LCZ concentration over time with varying amount of initial Salt Concentration in the LCZ:

4.5.(a) Comparison for Change in Concentration Profile over time with varying amount of initial Salt Concentration in the LCZ and with zero gradient boundary condition for concentration at the bottom boundary :

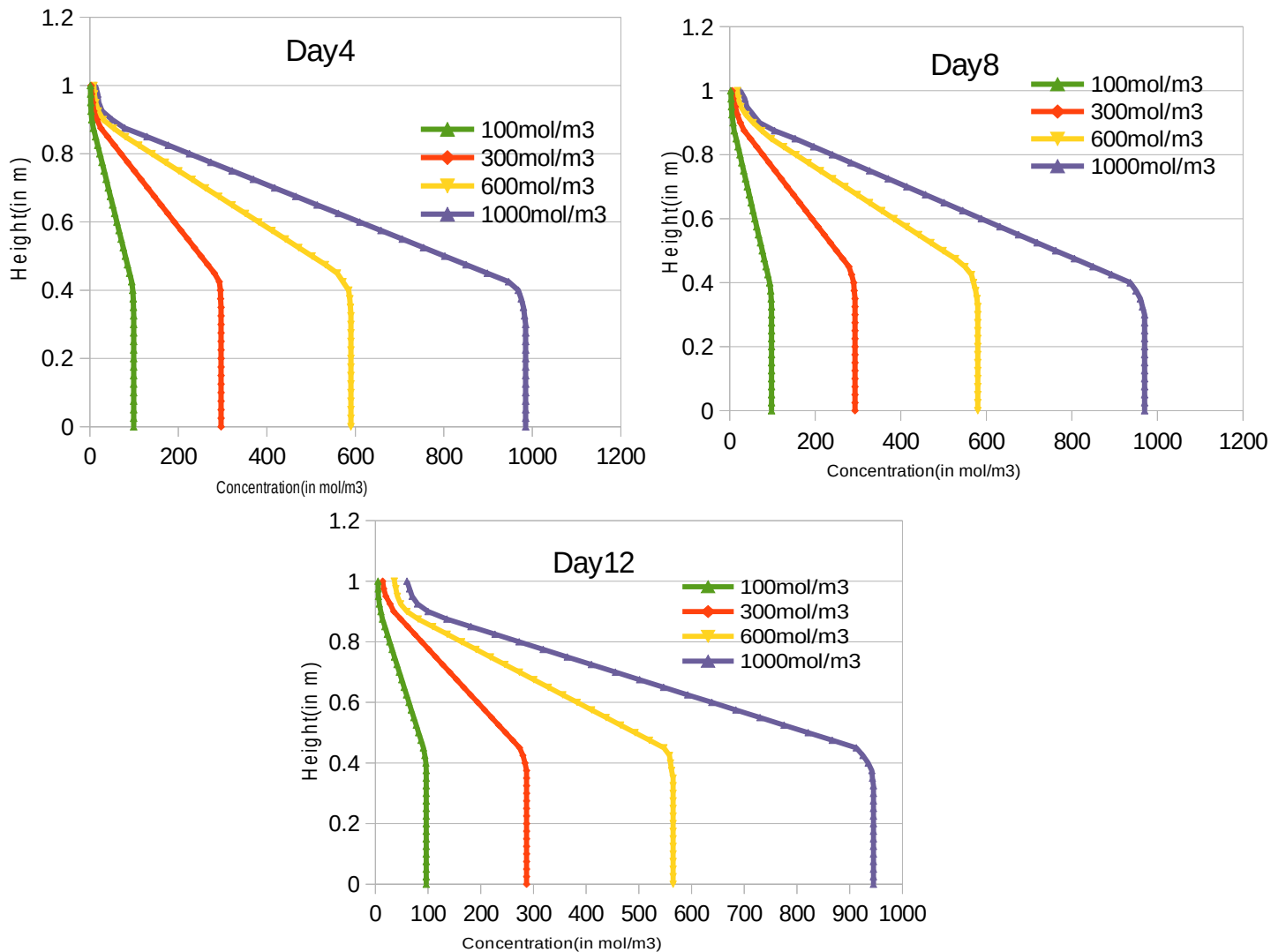


Figure 19(a). Change in Concentration Profile over time with varying amount of initial Salt Concentration in the LCZ and with zero gradient boundary condition for concentration at the bottom boundary.

The concentration profile and its subsequent change with time is a clear indication of the phenomena of diffusion taking place with very slight reduction of concentration in the lower convection zone and subsequently slight increase in the upper convection zone. The concentration gradient setup prevails convection current from generating inside the pond leading to mixing in the pond, and also as diffusion is slow process it takes a long time before complete mixing of the salt layers inside the pond. Both of the two factors allow for the salt gradient solar pond to be stable and the pond to remain use for a very long period of time. This ability of the concentration gradient to prevent mixing is due to the increased density in the lower layers, which when acted upon by gravity prevails prevent generation of convection currents and hence prevent mixing. As seen in Figure 19(a), with increased salt concentration in the LCZ, a steeper gradient is formed while with time the concentration in the LCZ gradually reduces over time, and consequently an increase in the UCZ. This Behaviour becomes more pronounced with the increase in initial LCZ concentration.

4.5.(b) Comparison for Change in Concentration Profile over time with varying amount of initial Salt Concentration in the LCZ and with fixed concentration boundary condition for concentration at the bottom boundary :

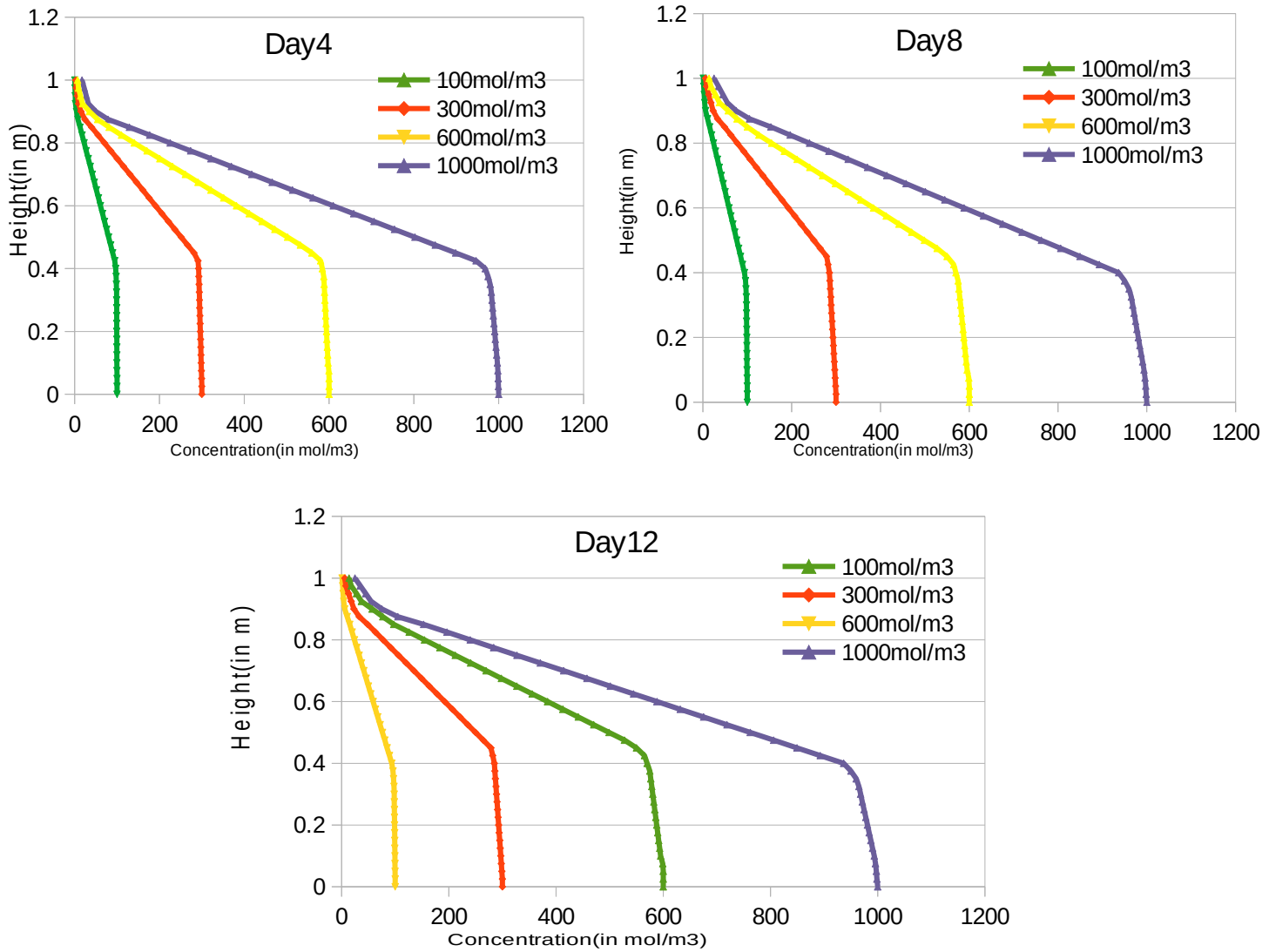
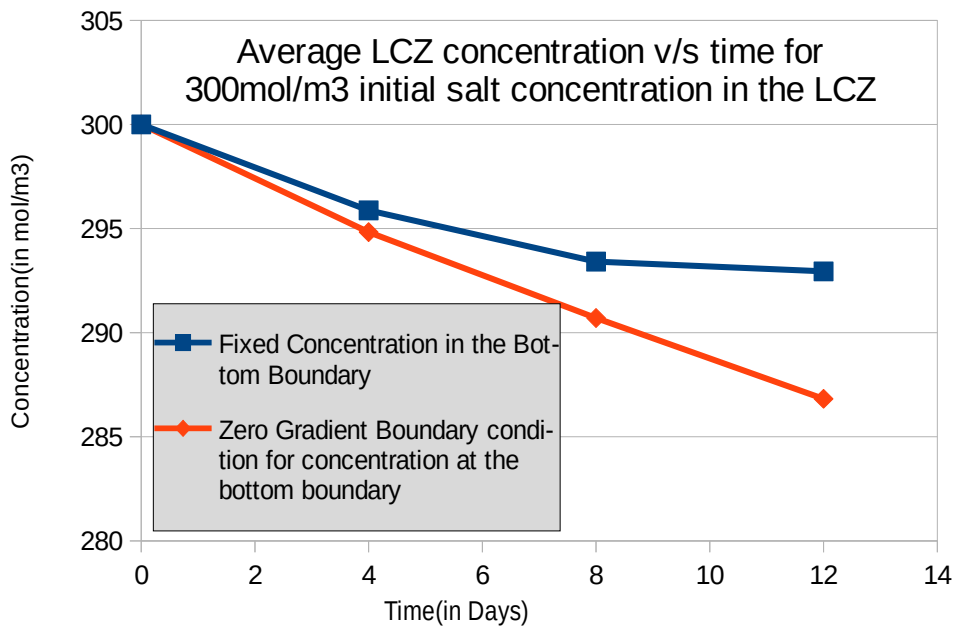
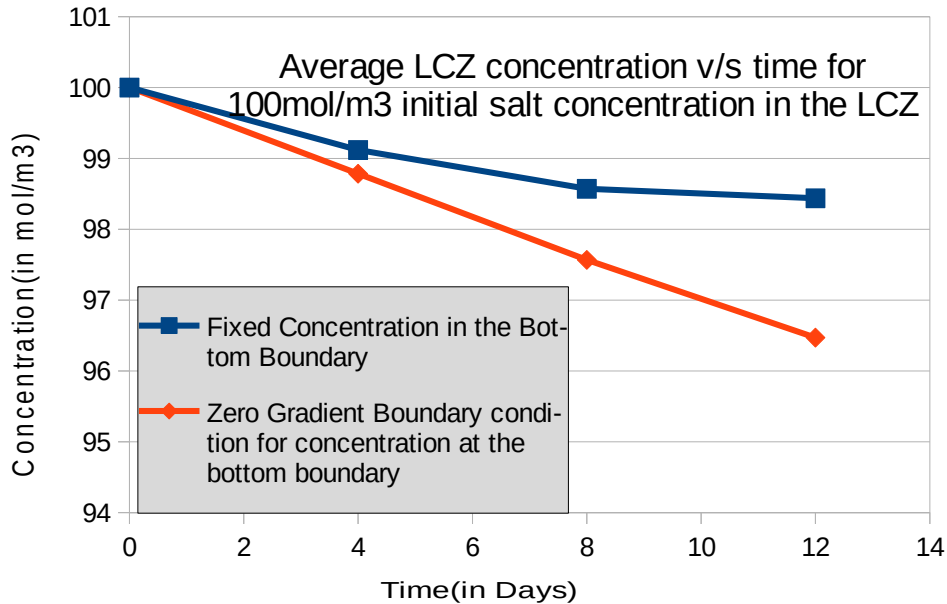


Figure 19(b). Change in Concentration Profile over time with varying amount of initial Salt Concentration in the LCZ and with fixed concentration boundary condition for concentration at the bottom boundary.

For the fixed boundary condition for concentration at the bottom, the bottom layer and layers immediately in the vicinity, stay at the value of the initial condition, and the subsequent extent of reduction and increase in the respective values of concentration in LCZ and UCZ is low. Also, it is seen that, the Concentration in the LCZ does not remain uniform throughout as with the case of zero gradient boundary condition for concentration at the bottom boundary in figure 19(a), with more reduction near the interface while it remains very close to the initial value at the bottom layer where the fixed concentration boundary condition has been implemented. This effect is more profound with increasing value of initial concentration of salt in LCZ. On comparing with zero gradient boundary condition for concentration at the bottom boundary, the runs with zero gradient condition show a reduction in the entire length of the LCZ which leads to greater diffusion of salt from LCZ to the UCZ over time. Also, the change in the salinity gradient is also more pronounced for cases with zero-gradient boundary condition for concentration at the bottom boundary.

4.5.(c) Comparison for Change in average LCZ concentration over time with varying amount of initial Salt Concentration in the LCZ and with fixed concentration boundary and zero gradient boundary condition condition for concentration at the bottom boundary :



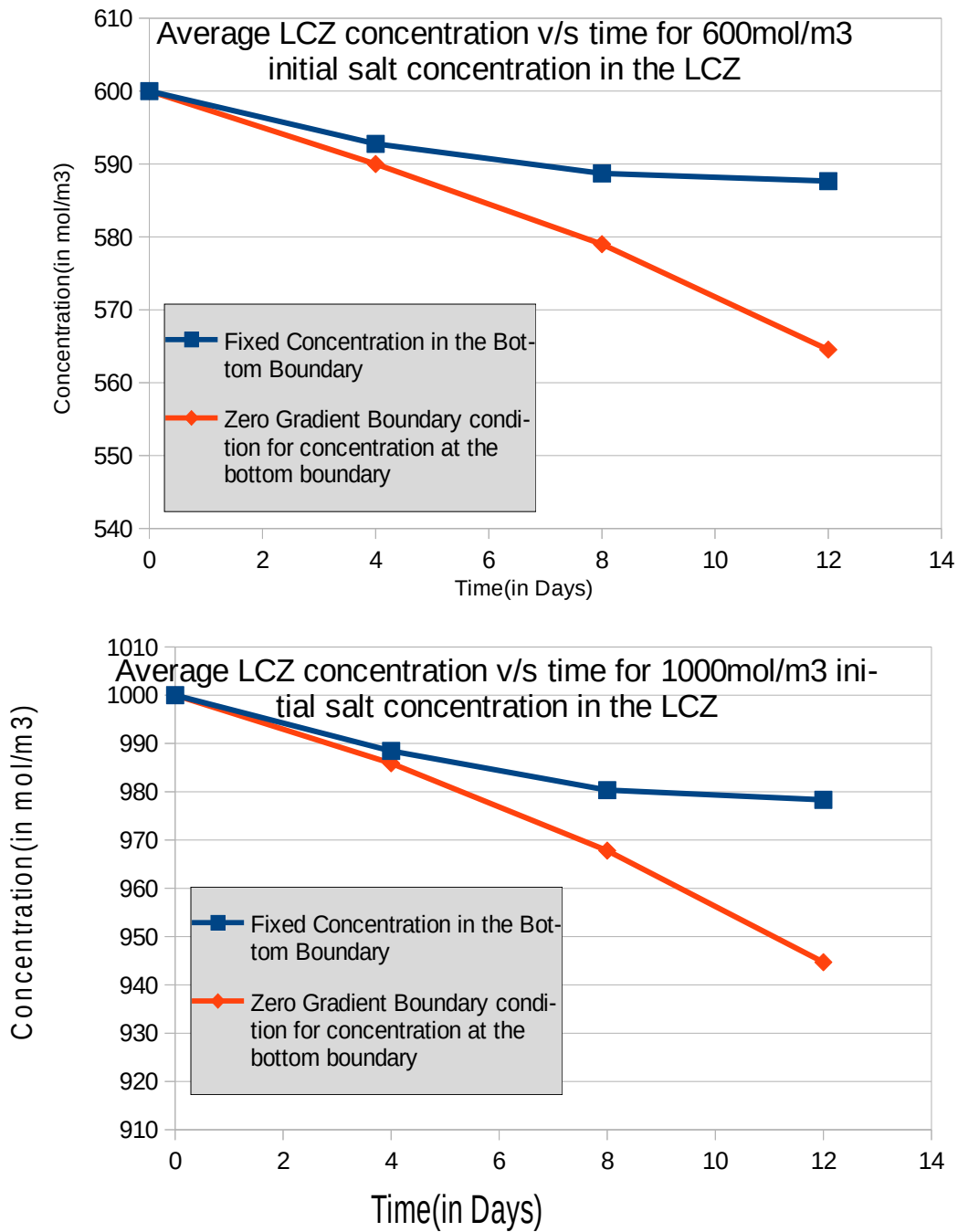


Figure 19(c). Change in average LCZ concentration over time with varying amount of initial Salt concentration, 100mol/m^3 , 300mol/m^3 , 600mol/m^3 , and 1000mol/m^3 , in the LCZ and with fixed concentration boundary condition and zero gradient boundary condition for concentration at the bottom boundary.

The average value for concentration in the LCZ reduces over time for all cases of varying values of initial salt concentration, however on comparing the two different boundary conditions the reduction in average concentration in the LCZ, due to diffusion from the LCZ is much slower with fixed concentration boundary condition at the bottom as compared to the zero gradient boundary condition. On comparing reduction of average LCZ concentration over time with data from Dah et. al., 2004 [30], for an actual Solar Pond, the zero gradient boundary condition for concentration at the bottom of the pond is more close to the behaviour of an a experimental SGSP as seen in Dah et. al., 2004 [30].

5. Conclusion:

In the study, a solver is developed in OpenFOAM, to solve the governing equations of a Salt Gradient Solar Pond(SGSP), the subsequent solvers capability is tested by operating on a model SGSP, which is a thin square of side 1m, with each zone namely, LCZ, NCZ and UCZ have been provided the height of 0.4m, 0.5m and 0.1m respectively. During the operation, certain assumptions have been made to simplify the process, as per [Ridha Boudihaf, et. al., 2015.\[29\]](#). For temperature, the walls on the side and bottom have been provided with zero-gradient boundary condition. The initial condition for Temperature has been specified as 293K. For Concentration, the side walls have been given the zero-gradient boundary condition, while two different boundary conditions have been tested for at the bottom. Also, Four different Concentration values in the LCZ have been considered as initial conditions, 100mol/m^3 , 300mol/m^3 , 600mol/m^3 and 1000mol/m^3 . For incident radiation, three values have been used, 250W/m^2 , 500W/m^2 and 1000W/m^2 at the pond surface . The radiation heat flux available at the depth is obtained by the correlation provided by Rabl and Nielsen, 1975[25], losses from the pond surface has been provided with values of 4W/m^2 for all values of incident radiation of 250W/m^2 , 500W/m^2 , and 1000W/m^2 , these values have been used as per loss in a SGSP during ambient condition of 293K as per M.R. Jaefarzadeh , 2004[27]. For every step of the simulation, it has been ensured to check on the Courant number to keep it below 1. On testing for grid convergence, a time step of 0.5 seconds and a Grid of 40x40 has been selected for each run.

While varying the incident radiation keeping the initial conditions fixed, it has been observed that with increasing values of incident radiation, the Temperature gradient established inside the pond becomes more steep, as per Figure 10(a), also it is seen that as time progresses, the gradient becomes more steep. Inside the LCZ, the average value of temperature increases with time as per Figure 10(b), with higher values of incident radiation leading to higher Temperature. Eventually the rate of increase of average temperature in the LCZ slows down, this is due to the loss value which is causing the pond to slowly move towards steady-state. The temperature profile attained, when considered at the interface of LCZ and NCZ the temperature profile for all cases of incident radiation is not sharp, this may be attributed due to mixing of temperatures at the interface.

On running for different values for Initial LCZ salt concentration, The Salt Gradient inside the pond in the NCZ gradually changes over time as per Figure 11(a) to 18(a), the change in the concentration profile is due to diffusion from LCZ to the UCZ, which results in gradual reduction of average LCZ concentration over time as per 11(b) to 18(b).

Two different bottom boundary conditions have been investigated for concentration, in one set zero gradient concentration boundary condition has been used as the bottom boundary condition, while in another set Fixed concentration condition has been used as bottom boundary condition, while comparing these two cases,

investigating the concentration profile it is observed that for Fixed concentration boundary condition at the bottom boundary, the bottom layer of the LCZ and layers immediately in the vicinity, stay at the value of the initial condition, and the subsequent extent of reduction and increase in the respective values of concentration in LCZ and UCZ is low, while in case of zero gradient boundary condition for concentration at the bottom boundary, the concentration reduces evenly through the entire length of the LCZ as per figure 19(a) and 19(b). Investigating the reduction of Average Concentration of the LCZ over time, figure 19(c), highlights that the diffusion of salt from the LCZ is reduced in case of fixed salt concentration condition as the bottom boundary condition.

The Solver has also been used to simulate Experimental Pond set ups, as per M.R. Jaefarzadeh , 2004[27], and also for Dah et. al., 2004 [30]. In both cases, upon providing the required initial values, operating conditions and boundary conditions, the results obtained are observed to be in accordance with the experimental results, Figure 5(a), 5(b) and 5(c) for comparison with M.R. Jaefarzadeh , 2004[27], and Figure 6(a) and 6(b), for Dah et. al., 2004 [30].

6.Nomenclature:

C Concentration of solution, (kg/m^3),

C_0 Reference Concentration of solution, (kg/m^3),

D Diffusion coefficient, (m^2/s),

$E(Z, t)$ solar radiation absorbed in the body of the pond ($\text{W}/\text{m}^2/\text{m}$)

h local time

h_s hour of sunrise

I solar radiation(W/m^2)

I_R direct radiation(W/m^2)

I_s radiation entering the pond surface (W/m^2)

L Length, (m),

LCZ Lower Convective Zone,

L_D the length of the day (hours)

n the day of the year, index of refraction

NCZ Non-convective zone,

Q_R total radiation energy entering into the LCZ(W)

R the coefficient of Reflection(dimensionless)

S Thermal source term

T Temperature, ($^{\circ}\text{C}$)

T_0 Reference Temperature, ($^{\circ}\text{C}$)

\vec{V} Velocity in (m/s)

UCZ Upper convective zone,

x, y horizontal and vertical coordinates, (m),

Greek symbols:

α Thermal diffusivity, (m^2/s),

β_T Thermal expansion coefficient, ($1/^{\circ}\text{C}$),

β_C Concentration expansion coefficient, (m^3/kg),

μ Dynamic viscosity, (kg/ms),

ρ Density, (kg/m^3),

ρ_0 Density at reference temperature T_0 and reference salt-concentration C_0

φ the angle of latitude,

θ_i the angle of incidence,

θ_r the angle of refraction

τ transmissivity(dimensionless)

Φ the angle of latitude

ω hour angle

δ angle of declination

7. Appendix of Data Used:

α Thermal diffusivity, (m^2/s) 1.3×10^{-7} [31]

D Diffusion coefficient, (m^2/s) 1.607×10^{-9} [32]

β_T Thermal expansion coefficient, ($1/\text{K}$) : 2.23×10^{-4} [33]

β_C Concentration expansion coefficient, (m^3/kg) : 7.81×10^{-4} [33]

μ Dynamic viscosity, (kg/ms) : 10^{-3}

8.References:

- [1]Tabor, H., 1981. Solar ponds. Sol. Energy 27, 181–194.
- [2]Tabor, H., 1980. Non-convecting solar ponds. Philos. Trans. R. Soc. A Math. Phys.Eng. Sci. 295, 423–433.
- [3]Osamah A.H. AL-Musawi, Anees A. Khadom, Hammed B. Manhood, Mustafa S. Mahdi., Solar pond as a low grade energy source for water desalination and power generation: a short review, Renew. Energy Environ. Sustain. 5 4 (2020)
- [4]Agha, K.R., Rice, G., Wheldon, A., 2001. The thermal characteristics and economic analysis of a solar pond coupled low temperature multi stage desalination plant part ii:economic analysis. Int. J. Sol. Energy 21, 1–18.
- [5]Hadi Rostamzadeh, Amin Shekari Namin, Pejman Nourani, Majid Amidpour, Hadi Ghaebi, Feasibility investigation of a humidification-dehumidification (HDH) desalination system with thermoelectric generator operated by a salinity-gradient solar pond, Desalination, Volume 462, 2019, Pages 1-18.
- [6]Sayantan Ganguly, Abhijit Date, Aliakbar Akbarzadeh, On increasing the thermal mass of a salinity gradient solar pond with external heat addition: A transient study,

Energy, Volume 168, 2019, Pages 43-56

[7]Beiki, H., Soukhtanlou, E. Determination of optimum insulation thicknesses for salinity gradient solar pond's bottom wall under different climate conditions. SN Appl. Sci. 2, 1284 (2020).

[8]Hua Wang, Xiaolei Yu, Feiling Shen, Liugang Zhang, A Laboratory experimental study on effect of porous medium on salt diffusion of salt gradient solar pond, Solar Energy, Volume 122, 2015,Pages 630-639.

[9]Hua Wang, Liu Gang Zhang, Yan Yang Mei, Investigation on the exergy performance of salt gradient solar ponds with porous media, Int. J. Exergy, Vol. 25, No. 1, 2018

[10]Giestas, M., Pina, H. and Joyce, A. (1996) 'The influence of radiation absorption on solar pond stability', Int. J. Heat Mass Transfer, Vol. 39, No. 18, pp.3873–3885.

[11]Hua Wang, Jianing Zou, J.L. Cortina, J. Kizito, Experimental and theoretical study on temperature distribution of adding coal cinder to bottom of salt gradient solar pond, Solar Energy, Volume 110, 2014, Pages 756-767.

[12]Mohamad Aramesh, Alibakhsh Kasaeian, Fathollah Pourfayaz, Dongsheng Wen,

Energy analysis and shadow modeling of a rectangular type salt gradient solar pond, Solar Energy, Volume 146, 2017, Pages 161-171.

[13]Asaad H. Sayer, Hazim Al-Hussaini, Alasdair N. Campbell, An analytical estimation of salt concentration in the upper and lower convective zones of a salinity gradient solar pond with either a pond with vertical walls or trapezoidal cross section, Solar Energy, Volume 158, 2017, Pages 207-217.

[14]Choubani Karim, Zitouni Slim, Charfi Kais, Safi Mohamed Jomâa, Aliakbar Akbarzadeh, Experimental study of the salt gradient solar pond stability, Solar Energy, Volume 84, Issue 1, 2010, Pages 24-31.

[15]Shyamal G. Chakrabarty, Uday S. Wankhede, Rupesh S. Shelke, Trushar B. Gohil, Investigation of temperature development in salinity gradient solar pond using a transient model of heat transfer, Solar Energy, Volume 202, 2020, Pages 32-44.

[16]V.V.N. Kishore, Veena Joshi, A practical collector efficiency equation for nonconvecting solar ponds, Solar Energy, Volume 33, Issue 5, 1984, Pages 391-395.

[17]Jeffrey A. Ruskowitz, Francisco Suárez, Scott W. Tyler, Amy E. Childress, Evaporation suppression and solar energy collection in a salt-gradient solar pond, Solar Energy, Volume 99, 2014, Pages 36-46.

- [18]Cristóbal Silva, Daniel González, Francisco Suárez, An experimental and numerical study of evaporation reduction in a salt-gradient solar pond using floating discs, *Solar Energy*, Volume 142, 2017, Pages 204-214.
- [19]Howard O. Njoku, Boniface E. Agashi, Samuel O. Onyegegbu, A numerical study to predict the energy and exergy performances of a salinity gradient solar pond with thermal extraction, *Solar Energy*, Volume 157, 2017, Pages 744-761.
- [20]Qi Wu, Hua Wang , Shukuan Xie, Liugang Zhang, Jie Wang, Zhanwei Dong and Tao Zhao, Effect of heat extraction on the thermal efficiency of salt gradient solar pond, *Energy Exploration & Exploitation*, 0(0), 2018.
- [21]Shahram Derakhshan, Seyedeh Elnaz Mirazimzadeh, Syamak Pazireh, Study of Buoyancy-Driven Flow Effect on Salt Gradient Solar Ponds Performance, *Journal of Energy Resources Technology*, 2018.
- [22]Khadije El Kadi, Sherine Elagroudy, Isam Janajreh, Flow simulation and Assessment of Salinity Gradient Solar Pond Development, *Energy Procedia* 158 (2019) 911–917.
- [23]Duffie, John A., and William A. Beckman. *Solar engineering of thermal processes*. New York: Wiley, 1980.

- [24]Y.F. Wang, A. Akbarzadeh, A parametric study on solar ponds, Solar Energy, Volume 30, Issue 6, 1983, Pages 555-562, ISSN 0038-092X, [https://doi.org/10.1016/0038-092X\(83\)90067-1](https://doi.org/10.1016/0038-092X(83)90067-1).
- [25]Ari Rabl, Carl E. Nielsen, Solar ponds for space heating, Solar Energy, Volume 17, Issue 1, 1975, Pages 1-12, ISSN 0038-092X, [https://doi.org/10.1016/0038-092X\(75\)90011-0](https://doi.org/10.1016/0038-092X(75)90011-0).
- [26]Akbarzadeh, A.A., Ahmadi, G., 1980. Computer simulation of the performance of a solar pond in the southern part of Iran. Solar Energy 24, 143–151.
- [27]M.R. Jaefarzadeh, Thermal behavior of a small salinity-gradient solar pond with wall shading effect, Solar Energy, Volume 77, Issue 3, 2004, Pages 281-290, ISSN 0038-092X, <https://doi.org/10.1016/j.solener.2004.05.013>.
- [28]Manu Chakkingal, Roland Voigt, Chris R. Kleijn, Saša Kenjereš, Effect of double-diffusive convection with cross gradients on heat and mass transfer in a cubical enclosure with adiabatic cylindrical obstacles, International Journal of Heat and Fluid Flow, Volume 83, 2020.
- [29]Boudhiaf, R. Numerical temperature and concentration distributions in an insulated salinity gradient solar pond. Renewables 2, 10 (2015).

<https://doi.org/10.1186/s40807-015-0011-3>

[30]Dah, Mohamed El Mokhtar & Ouni, M. & Guizani, A. & Belghith, Abdelfettah. (2004). Experimental study of the evolution of temperature and salinity profiles in a salinity gradient solar pond. 10.13140/2.1.1031.9689.

[31]Kaufmann, D.W., 1960. Sodium Chloride. Reinhold, New York.

[32]UKEssays. (November 2018). Diffusion Coefficient of 2m NACL in Water. Retrieved from <https://www.ukessays.com/essays/biology/measurement-of-liquid-diffusion-coefficient-biology-essay.php?vref=1>

[33]The international thermodynamic equation of seawater – 2010: Calculation and use of thermodynamic properties,
http://www.teos-10.org/pubs/TEOS-10_Manual.pdf